INTERNATIONAL ATOMIC ENERGY AGENCY
UNITED NATIONS EDUCATIONAL, SCIENTIFIC AND CULTURAL ORGANIZATION
INTERNATIONAL CENTRE FOR THEORETICAL PHYSICS
I.C.T.P., P.O. BOX 586, 34100 TRIESTE, ITALY, CABLE: CENTRATOM TRIESTE

H4.SMR/782-8

Second Workshop on
Three-Dimensional Modelling of Seismic Waves
Generation, Propagation and their Inversion

7 - 18 November 1994

Long Period Seismology and the Earth's Free Oscillations

J.H. Woodhouse

Department of Earth Sciences
Oxford University
Oxford, U.K.

Long period Seismology and the Earth's Free Oscillations

J. H. Woodhouse
Department of Earth Sciences, Oxford University
Parks Road, Oxford OX1 3PR, U.K.

1 Introduction

In these lectures we shall aim to present some of the theoretical background which is necessary to pursue long period studies in seismology. Seismograms, which represent ground acceleration as a function of time at a given seismic station, are most readily understood at relatively low frequencies (periods longer than about 30s, say) because the influence of aspherical structure is smaller. For example, a travel time anomaly of several seconds may correspond, for long period data, to an offset in phase of a small fraction of a cycle. In short period data, on the other hand, such a delay time anomaly may offset the waveform by many cycles. In the former case there is some hope of determining adjustments to the Earth model which will bring data and theoretical seismograms into phase agreement, by means of perturbation theory and inversion of the data. In the short period case there is little hope of achieving this, since the corresponding inverse problem is highly nonlinear. Instead, in the short period case, one is limited to measuring the travel time delay and then seeking to improve the model so that the delay is more accurately predicted. Thus, there have developed two basic kinds of tomography which might be termed 'waveform tomography' and 'delay time tomography'. Within these there are a number of different approaches, making use of different spectral and temporal domains, different algorithms for the evaluation of theoretical seismograms, different model parameterizations etc. The information provided by the two aproaches is complementary and, indeed, many of the results of tomography have been reproduced using very different kinds of data and modelling techniques.

2 Equations of linear elasicity with gravitation and initial stress

Seismic waves in the Earth are governed, in the first approximation, by the linear theory of elasticity; the attenuation or damping of seismic waves is well described in terms of a linearly viscoelastic rheology, and only in the vicinity of earthquake sources do we expect major departures from these relatively simple mechanical descriptions. In the Earth the presence of an initial stress field and self gravitation must also be taken into account. Here we review some of the basic elements of the theory of elasticity in the presence of gravitation and and an initial stress distribution. For the case in which the

initial stress field is a simply a radially dependent hydrostatic pressure $p^0(r)$, and where the elastic constituive law is isotropic, the equations have long been known (see e.g. Love, 1911, Pekeris and Jarosch, 1958). For the general case, in which there is a non-hydrostatic initial stress field $t_{ij}^{(0)}$, correct statements of the equations are by Dahlen and Smith (1975), Woodhouse and Dahlen (1978), Valette (1986). Earlier treatments (Dahlen, 1972, 1973) give the conceptual basis, using the results of Biot (1965), but were marred by certain algebraic errors; the treatment by Geller (1988) suffers from major conceptual errors. The effects of non-hydrostatic initial stress have not been observed and are invariably neglected; from the theoretical point of view, however, it is of interest to write down the completely general equations.

We shall use a fixed Cartesian set of axes and express all vectors and tensors in terms of their components with respect to these axes. Later we shall also make use of spherical coordinates (r, θ, ϕ) defined through

$$\mathbf{x} = (r\sin\theta\cos\phi, r\sin\theta\sin\phi, r\cos\theta) \tag{2.1}$$

Consider a material which is initially in equilibrium under self-gravitation. The equations of mechanical equilibrium and gravitation may be written

$$t^0_{ij,j} = \rho^0\phi^0_{,i} \tag{2.2}$$

$$\phi_{,ii} = 4\pi G\rho^0 \tag{2.3}$$

where t^0_{ij} is the initial stress field, ϕ^0 is the initial gravitational potential and ρ^0 is the initial density, all of which are functions of position $\mathbf{x}$, and where G is the gravitational constant; the notation $\phi_{,i}$ *etc.* denotes differentiation with respect to x_i and summation over repeated indices is assumed. Upon deformation, the material particle initially at any point $\mathbf{x}$ moves to the point $\mathbf{r} = \mathbf{r}(\mathbf{x}, t)$, where t is time. The stress tensor and the gravitational potential will now be functions of space and time coordinates; they may be regarded either as functions of the current coordinates, r_i say, or as functions of the initial coordinates of the particle currently at r_i, which we denote by x_i, with the understanding that x_i and r_i are related by the deformation $\mathbf{r} = \mathbf{r}(\mathbf{x}, \mathbf{t})$. The momentum equation and the law of gravitation can be written:

$$\frac{\partial t_{ij}}{\partial r_j} = \rho\frac{\partial\phi}{\partial r_i} + \rho\ddot{r}_i \tag{2.4}$$

$$\frac{\partial}{\partial r_i}\frac{\partial\phi}{\partial r_i} = 4\pi G\rho \tag{2.5}$$

or

$$x_{kj}t_{ij,k} = \rho x_{ki}\phi_{,k} + \rho\ddot{r}_i \tag{2.6}$$

$$x_{ki}(x_{li}\phi_{,l})_{,k} = 4\pi G\rho \tag{2.7}$$

where

$$x_{ki} = \frac{\partial x_k}{\partial r_i} \; . \tag{2.8}$$

Note that we reserve the notation $\phi_{,i}$ *etc.* for derivatives with respect to x_i; '$\cdot$' denotes the time derivative at constant $\mathbf{x}$ – i.e. the material time derivative. Since mass is conserved, the mass of a deformed volume element d^3r must be equal to that of the corresponding undeformed element d^3x; *i.e.* $\rho d^3r = \rho^0 d^3x$ and thus

$$J\rho = \rho^0 \tag{2.9}$$

where J is the Jacobian

$$J = J(\mathbf{x}) = \frac{\partial(r_1, r_2, r_3)}{\partial(x_1, x_2, x_3)} \ . \tag{2.10}$$

Let us now write

$$r_i = x_i + u_i \tag{2.11}$$

where u_i is small, and define the first order quantities ρ^1 and ϕ^1 to be the change in density and gravitational potential, at a fixed point in space, due to the deformation. Also we define t^1_{ij} to be the change in stress at a material particle. We may write

$$t^1_{ij} = t_{ij}(\mathbf{r}) - t^0(\mathbf{x}) \tag{2.12}$$
$$\rho^1 = \rho(\mathbf{r}) - \rho^0(\mathbf{r}) \tag{2.13}$$
$$\phi^1 = \phi(\mathbf{r}) - \phi^0(\mathbf{r}) \tag{2.14}$$

whence

$$t_{ij} = t_{ij}(\mathbf{r}) = t^0_{ij} + t^1_{ij} \tag{2.15}$$
$$\rho = \rho(\mathbf{r}) = \rho^0(\mathbf{x}+\mathbf{u}) + \rho^1 = \rho^0 + u_k\rho^0_{,k} + \rho^1 \tag{2.16}$$
$$\phi = \phi(\mathbf{r}) = \phi^0(\mathbf{x}+\mathbf{u}) + \phi^1 = \phi^0 + u_k\phi^0_{,k} + \phi^1 \tag{2.17}$$

Making use of the first order approximation

$$J = \det(r_{i,j}) = \det(\delta_{ij} + u_{i,j}) = 1 + u_{j,j} \tag{2.18}$$

in (2.9) and (2.16), we also find

$$\rho^0 = (1 + u_{j,j})(\rho^0 + u_k\rho^0_{,k} + \rho^1) \tag{2.19}$$

and thus, from the first order terms:

$$\rho^1 = -u_k\rho^0_{,k} - \rho^0 u_{k,k} = -(\rho^0 u_k)_{,k} \ . \tag{2.20}$$

In order to complete the system of equations of motion we need to specify the constitutive law giving the incremental stress t^1_{ij} in terms of the elastic displacement field u_i. The correct form for this relationship depends upon the hypothesis that there exits an internal energy density function $E(\mathbf{x}, \mathbf{e}, s)$ (per unit undeformed volume or, equivalently, per unit mass), where $\mathbf{e}$ is the (exact) strain tensor:

$$e_{ij} = \tfrac{1}{2}(r_{k,i}r_{k,j} - \delta_{ij}) \tag{2.21}$$

and s is specific entropy. Here we shall be concerned only with isentropic deformations and shall not consider further any thermodynamic quantities. This is appropriate for the Earth since thermal fluctuations propagate on timescales vastly greater than the periods of seismic waves. The implications of the existence of an internal energy density function have to be worked out to second order in order to obtain the correct incremental constitutive law; the derivation is somewhat too lengthy to be included here. A very complete discussion is contained in the monograph by Biot (1965); see also the papers by Dahlen (1972, 1973), Dahlen and Smith (1975), Woodhouse and Dahlen (1978) and Valette (1986). The result is that t^1_{ij} can be written:

$$t^1_{ij} = c_{ijkl}u_{k,l} + t^0_{jk}u_{i,k} + t^0_{ik}u_{j,k} - t^0_{ij}u_{k,k} \tag{2.22}$$

where the fourth rank tensor $\mathbf{c} = \mathbf{c}(\mathbf{x})$ posesses the symmetries:

$$c_{ijkl} = c_{jikl} = c_{klij} \ . \tag{2.23}$$

Following Dahlen and Smith (1975) and Woodhouse and Dahlen (1978) we define

$$\Lambda_{jilk} = c_{ijkl} + t^0_{jl}\delta_{ik} \tag{2.24}$$

and write

$$t^1_{ij} = \Lambda_{jilk}u_{k,l} + t^0_{ik}u_{j,k} - t^0_{ij}u_{k,k} \ . \tag{2.25}$$

The first term on the right side of (2.25) is the incremental Piola-Kirchhoff stress tensor (see e.g. Malvern, 1969).

We now substitute into the exact equations of motion (2.6), (2.7) the first order approximations (2.15), (2.16), (2.17), together with (2.20) and (2.25) and the first order relation:

$$x_{ij} = \delta_{ij} - u_{i,j} \tag{2.26}$$

to obtain the equations satisfied by $\mathbf{u}$ and ϕ^1. On simplification we find:

$$\rho^0(\ddot{u}_i + \phi^1_{,i} + \phi^0_{,j}u_j) = (\Lambda_{jilk}u_{l,k})_{,j} \tag{2.27}$$

$$\phi^1_{,ii} = -4\pi G(\rho^0 u_i)_{,i} \ . \tag{2.28}$$

The Earth consists of a number of regions – inner core, core, lower mantle, upper mantle etc. within each of which material properties, it is assumed, are smooth fuctions of position. Within each region the equations of motion (2.27), (2.28) must be satisfied; across the boundaries separating the regions certain conditions, ensuring the continuity of traction, gravitational potential and its derivatives and, where appropriate, continuity of displacement are required. Here we shall only state them – see Woodhouse and Dahlen (1978) for a detailed discussion. We identify three kinds of boundaries: *welded*, – *e.g.* the boundary between the upper mantle and the lower mantle at approximately

670 km depth and the Mohorovicic discontinuity; *free slip* – the inner core boundary, the core-mantle boundary and the ocean floor; and *free* – the ocean surface or, in the absence of an ocean, the outer surface of the solid Earth. Also, the gravitational potential is required to vanish at infinity. The complete set of boundary conditions is as follows:

$$\begin{aligned}
&\text{Welded:} && [u_i]^+_- = 0 && (2.29)\\
& && [t_i]^+_- = 0 && (2.30)\\
&\text{Free-slip:} && [n_i u_i]^+_- = 0 && (2.31)\\
& && [t_i]^+_- = 0 && (2.32)\\
& && t_i = n_i n_j t_j && (2.33)\\
&\text{Free:} && t_i = 0 && (2.34)\\
&\text{All:} && [\phi^1]^+_- = 0 && (2.35)\\
& && [\phi^1_{,i} n_i + 4\pi G \rho^0 u_i n_i]^+_- = 0 && (2.36)\\
&\text{Infinity:} && \phi^1 = 0 && (2.37)
\end{aligned}$$

in which $\mathbf{n}$ is the unit normal to the boundary and

$$t_i = \Lambda_{jilk} u_{l,k} n_j - n_i \nabla^1_k (\pi^0 u_k) + \pi^0 n_k \nabla^1_i u_k \ , \tag{2.38}$$

where

$$\pi^0 = t^0_{ij} n_i n_j \tag{2.39}$$

and where $\boldsymbol{\nabla}^1$ is the surface gradient operator

$$\boldsymbol{\nabla}^1 = \boldsymbol{\nabla} - \mathbf{nn} \cdot \boldsymbol{\nabla} \ . \tag{2.40}$$

Equations (2.27 – 2.37) are to be regarded as governing the four unknown fields $u_i(\mathbf{x}, t)$, $\phi^{(1)}(\mathbf{x}, t)$, which represent possible *free* oscillations of the Earth. All other quantities: ρ^0, t^0_{ij}, ϕ^0, Λ_{jilk} are regarded as given parameters of the earth model, subject to the equilibrium equations (2.2, 2.3) and the requirement that ϕ^0, $\phi^0_{,i}$, $t^0_{ij} n_j$ be continuous at all boundaries and that ϕ^0 vanishes at infinity.

In order to represent the excitation of the modes we introduce a specified force distribution $\mathbf{F}(\mathbf{x}, t)$ on the right hand side of (2.27) and write

$$\rho^0 (\ddot{u}_i + \phi^1_{,i} + \phi^0_{ij} u_j) - (\Lambda_{jilk} u_{l,k})_{,j} = F_i \tag{2.41}$$

The force distribution $\mathbf{F}$ is known as the equivalent body force distribution of the source. In order to represent an indiginous earthquake or explosion $\mathbf{F}$ must have the form (Backus and Mulcahy, 1976):

$$F_i = -\Gamma_{ij,j} \tag{2.42}$$

where $\boldsymbol{\Gamma} = \boldsymbol{\Gamma}(\mathbf{x}, t)$ is the *stress glut*, which represents the failure of the constitutive law (2.25, 2.38) to be satisfied in the source region. $\boldsymbol{\Gamma}$ has the important property that

it vanishes outside the source region and its time derivative vanishes both before the source origin time and after the source has ceased to act. Thus the *stress glut rate* $\dot{\Gamma}$ is nonzero only in the finite region of space and time corresponding to action of the source.

The equations and boundary conditions governing ϕ^1 can be solved for ϕ^1 in terms of $\mathbf{u}$. In fact ϕ^1 is the gravitational potential due to the density distribution $\rho^1 = -(\rho^0 u_k)_{,k}$ together with mass distributions on spherical boundaries having surface density $-[\rho^0 u_r]^+_-$. Thus it is convenient to regard $\phi^1(\mathbf{x}, t)$ as a functional of $\mathbf{u}(\mathbf{x}, t)$:

$$\phi^1 = \Phi[\mathbf{u}] \tag{2.43}$$

. The remaining equations, now governing only $\mathbf{u}$ can be written, symbolically:

$$(\mathcal{H} + \rho^0 \partial_t^2)\mathbf{u} = \mathbf{F} \tag{2.44}$$

where $\mathcal{H}$ represents the integro-differential operator corresponding to the left side of (2.41), in which ϕ^1 is replaced by $\Phi[\mathbf{u}]$, and also thought of as incorporating the boundary conditions (2.29–2.37).

3 Oscillations of a spherically symmetric Earth model

A useful approximate model of the Earth is one which is non-rotating, perfectly spherical and in equilibrium with a hydrostatic stress field

$$t^0_{ij} = -\delta_{ij} p^0(r) \tag{3.1}$$

where $p^0(r)$ is the initial pressure distribution. In this case the above general system of equations simplify greatly, and are separable in spherical coordinates. Thus they are amenable to solution by reduction to ordinary differential equations. Deviations from this model are relatively small in the Earth, and thus perturbation theory can be used to incorporate the effects of rotation, ellipticity and other asphericity, or more complex initial stress fields.

Under the assumption of hydrostatic initial stress and spherical symmetry the equilibrium equations (2.2, 2.3), together with the appropriate boundary conditions (see above) can be solved to determine ϕ^0, p^0 in terms of the given density distribution $\rho(r)$. We have:

$$g^0(r) = \partial_r \phi^0(r) = \frac{4\pi G}{r^2} \int_0^r \rho^0(r) r^2 dr \tag{3.2}$$

$$\phi^0(r) = -\int_r^\infty g^0(r) dr \tag{3.3}$$

$$= -\frac{GM}{a} - \int_r^a g^0(r) dr \tag{3.4}$$

$$p^0(r) = \int_r^a \rho^0(r) g^0(r) dr \tag{3.5}$$

where a is the radius of the Earth and M is the Earth's total mass:

$$M = 4\pi \int_0^a r^2 \rho^0(r) dr \tag{3.6}$$

When (3.1) is used in (2.22), (2.24), we obtain

$$t^1_{ij} = C_{ijkl} u_{k,l} \tag{3.7}$$

with

$$C_{ijkl} = c_{ijkl} - p^0(\delta_{jl}\delta_{ik} + \delta_{il}\delta_{jk} - \delta_{ij}\delta_{kl}) \tag{3.8}$$

$$A_{jilk} = C_{ijkl} + p^0(\delta_{il}\delta_{jk} - \delta_{ij}\delta_{kl}) \tag{3.9}$$

and on using (3.9) in (2.41) the equation of motion becomes:

$$\rho^0 \ddot{u}_i + \rho^0 \phi^1_{,i} - (\rho^0 u_j)_{,j} \phi^0 - (u_j p^0_{,j})_{,i} - (C_{ijkl} u_{k,l})_{,j} = F_i \tag{3.10}$$

Also, because of spherical symmetry C_{ijkl} cannot be arbitrary but must represent a tensor field invariant under rotations of the model. The most general form for such a tensor satisfying (2.23) depends upon just five scalar parameters (see e.g. Takeuchi and Saito, 1972) $A(r)$, $C(r)$, $F(r)$, $L(r)$, $N(r)$. Denoting the spherical components of $\mathbf{C}$ by C_{rrrr} $C_{rr\theta\theta}$ etc. the nonvanishing elements of $\mathbf{C}$ can be represented as:

$$C_{rrrr} = C(r) \tag{3.11}$$

$$C_{rr\theta\theta} = C_{rr\phi\phi} = C_{\theta\theta rr} = C_{\phi\phi rr} = F(r) \tag{3.12}$$

$$C_{\theta\theta\phi\phi} = C_{\phi\phi\theta\theta} = A(r) - 2N(r) \tag{3.13}$$

$$C_{\theta\phi\theta\phi} = C_{\phi\theta\theta\phi} = C_{\theta\phi\phi\theta} = C_{\phi\theta\phi\theta} = N(r) \tag{3.14}$$

$$C_{\phi r\phi r} = C_{r\phi\phi r} = C_{\phi rr\phi} = C_{r\theta r\theta} = L(r) \tag{3.15}$$

$$C_{\theta\theta\theta\theta} = C_{\phi\phi\phi\phi} = A(r) \tag{3.16}$$

In the case of *isotropy* we have:

$$A = C = \lambda + 2\mu = \kappa + \frac{4}{3}\mu \tag{3.17}$$

$$N = L = \mu \tag{3.18}$$

$$F = \lambda = \kappa - \frac{2}{3}\mu \tag{3.19}$$

where $\lambda = \lambda(r)$, $\mu = \mu(r)$ are the Lame parameters, $\kappa = \kappa(r)$ is bulk modulus and μ is shear modulus. In this case:

$$C_{ijkl} = \mu(\delta_{ik}\delta_{jl} + \delta_{il}\delta_{jk}) + \lambda\delta_{ij}\delta_{kl}. \tag{3.20}$$

In fluid regions we have:

$$N = L = \mu = 0 \tag{3.21}$$

$$C = A = F = \lambda = \kappa. \tag{3.22}$$

The boundary conditions on $\mathbf{u}$, ϕ^1 for this spherical model may be stated as folows:

Welded:	$[u_i]^+_- = 0$	(3.23)
	$[C_{ijkl}\hat{r}_j u_{k,l}]^+_- = 0$	(3.24)
Fluid-solid:	$[u_r]^+_- = 0$	(3.25)
	$[C_{ijkl}\hat{r}_j u_{k,l}]^+_- = 0$	(3.26)
Free:	$C_{ijkl}\hat{r}_j u_{k,l} = 0$	(3.27)
All:	$[\phi^1]^+_- = 0$	(3.28)
	$[\partial_r \phi^1 + 4\pi G\rho^0 u_r]^+_- = 0$	(3.29)
Infinity:	$\phi^1 = 0$	(3.30)

where $\hat{\mathbf{r}}$ is a unit vector in the direction of r increasing and where the square bracket notation is used to denote the discontinuity of the enclosed quantity across a surface of discontinuity in the model, the contribution from outside the surface being taken positive.

As in the general case (2.44) the problem of determining the seismic displacement in a spherical earth model can be written:

$$(\mathcal{H} + \rho^0 \partial_t^2)\mathbf{u} = \mathbf{F} \tag{3.31}$$

Taking the Fourier transform in time:

$$\overline{\mathbf{u}}(\mathbf{x},\omega) = \int_{-\infty}^{\infty} \mathbf{u}(\mathbf{x},t)e^{-i\omega t}dt \tag{3.32}$$

we have

$$(\mathcal{H} - \rho^0\omega^2)\overline{\mathbf{u}} = \overline{\mathbf{F}} \tag{3.33}$$

and thus, in order to determine $\overline{\mathbf{u}}$ we need to invert the operator represented on the left hand side. A natural way to proceed is to represent the solution in terms of the eigenfunctions $\mathbf{s}_k(\mathbf{x})$ satisfying:

$$\mathcal{H}\mathbf{s}_k = \rho^0\omega_k^2\mathbf{s}_k \qquad (k = 1,2,...\infty) \tag{3.34}$$

where ω_k^2 are the eigenvalues. It is clear that the function

$$\mathbf{u}(\mathbf{x},t) = e^{i\omega_k t}\mathbf{s}_k(\mathbf{x}) \tag{3.35}$$

satisifies (3.31) in the case $\mathbf{F} = \mathbf{0}$ and thus $\mathbf{s}_k(\mathbf{x})$ represents the spatial shape of a free oscillation of the model having angular frequency ω_k. It may be shown that the operator $\mathcal{H}$ is self adjoint in the sense

$$\int_V \mathbf{s}'.\mathcal{H}\mathbf{s}d^3x = \int_V \mathbf{s}.\mathcal{H}\mathbf{s}'d^3x \tag{3.36}$$

for any differetiable $\mathbf{s}(\mathbf{x})$, $\mathbf{s}'(\mathbf{x})$ satisfying the boundary conditions (3.23 – 3.27) and where the volume integration is over the entire earth model. From this it follows that the eigenfunctions $\mathbf{s}_k(\mathbf{x})$ form a complete set and that the eigenvalues ω_k^2 are real. Furthermore, if any of the eigenvalues is negative it follows that there exist exponentially growing solutions of the homogeneous equations (3.31). The existence of such solutions would indicate that the equilibrium configuration of the earth model was unstable. Since this would clearly be unrealistic we conclude that all of the ω_k are real, provided that we demand that the model is in stable equilibrium. In addition it is not difficult to show that eigenfunctions belonging to different eigenvalues are orthogonal or, in the case of degeneracy, can be orthogonalised, in the sense

$$\int_V \rho^0 \mathbf{s}_{k'}^* \cdot \mathbf{s}_k d^3x = 0 \qquad (k \neq k') \tag{3.37}$$

Using these results it is straightforward to obtain a formal solution of the forced equations of motion (3.31) in terms of a sum of eigenfunctions $\mathbf{s}_k$. We write:

$$\mathbf{u}(\mathbf{x},t) = \sum_k a_k(t)\mathbf{s}_k(\mathbf{x}). \tag{3.38}$$

On substituting into (3.31), multiplying by $\mathbf{s}_{k'}^*$ and integrating, making use of the orthogonality relation (3.37), we obtain

$$\ddot{a}_k(t) + \omega_k^2 a_k(t) = F_k(t) \tag{3.39}$$

with

$$F_k(t) \equiv \frac{\int_V \mathbf{s}_k^*(\mathbf{x}) \cdot \mathbf{F}(\mathbf{x},t) d^3x}{\int_V \rho_0 \mathbf{s}_k^*(\mathbf{x}) \cdot \mathbf{s}_k(\mathbf{x}) d^3x}. \tag{3.40}$$

The ordinary differential equations (3.39) for each $a_k(t)$ may be solved (e.g. using the method of *variation of parameters*, or Green's functions, or Laplace or Fourier transformation) to give

$$a_k(t) = \frac{1}{\omega_k^2} \int_{-\infty}^{t} h_k(t-t') \dot{F}_k(t') dt' \tag{3.41}$$

with

$$h_k(t) = 1 - \cos \omega_k t \tag{3.42}$$

a result originally due to Gilbert (1971). As pointed out by Gilbert (1971) this result needs to be modified to account for attenuation by incorporating a decay factor $\exp(-\alpha_k t)$ into the cosine term, and thus in place of (3.42) we write:

$$h_k(t) = 1 - e^{-\alpha_k t} \cos \omega_k t \tag{3.43}$$

In fact a more careful analysis, similar to that of the excitation of a damped simple harmonic oscillator, yields a slightly different result, not given here, which is well approximated by (3.43) in the case of realistically small α_k. The decay rate of the free oscillations is also often quantified by 'the Q of the mode' Q_k, which is defined in such a way that the amplitude decays by a factor $\exp(-\pi/Q_k)$ per period $(= 2\pi/\omega_k)$. Consequently Q_k and α_k are related by:

$$\alpha_k = \frac{\omega_k}{2Q_k}. \tag{3.44}$$

Making use of (3.41) in (3.38) we obtain an explicit expression for the theoretical seismogram. It is often sufficient to consider the case of a *point source* by which we shall mean a source having spatial and temporal extent small compared to the wavelengths and a periods of interest. In this case it may be shown (Backus and Mulcahy, 1976) that the expression (3.41) can be approximated by the simpler form:

$$a_k(t) = h_k(t - t_s) M_{ij} e_{ij}^{(k)*}(\mathbf{x}_s) \tag{3.45}$$

where $(\mathbf{x}_s, t_s)$ denote the spatial and temporal *centroid* of the source and where the symmetric tensor M_{ij}, the source *moment tensor*, is given by:

$$M_{ij} = \int_{-\infty}^{\infty} \int_V \dot{\Gamma}_{ij} d^3x dt \tag{3.46}$$

In (3.45) $e_{ij}^{(k)}$ denotes the strain in the k-th mode $e_{ij}^{(k)} = \frac{1}{2}(s_{i,j}^{(k)} + s_{j,i}^{(k)})$. For further details we refer to the review by Dziewonski and Woodhouse (1983) and to the literature already cited. Using (3.45) in (3.38) we obtain the following expression for a theoretical seismogram in a spherically symmetric model:

$$\mathbf{u}(\mathbf{x}, t) = \sum_k [1 - e^{-\alpha_k(t-t_s)} \cos \omega_k (t - t_s)] M_{ij} e_{ij}^{(k)*}(\mathbf{x}_s) \mathbf{s}_k(\mathbf{x}). \tag{3.47}$$

In order to apply this and earlier formulae in this section we need to have calculated a complete set of eigenfunctions $\mathbf{s}_k(\mathbf{x})$ together with the corresponding eigenfrequencies ω_k and attenuation constants α_k. For this we refer to the literature, only quoting the most important results. A thorough treatment is given by Takeuchi and Saito (1972). Woodhouse (1988) describes an algorithm for finding all modes, depending on an extension of Sturm-Liouville theory. A review of some of the salient points, together with expressions for the excitation coefficients are given by Dziewonski and Woodhouse (1983), citing earlier literature. Phinney and Burridge (1973) introduce a set of *generalized spherical harmonics* which enable any tensor field to be readily expanded in spherical harmonics. These greatly facilitate the derivation of the modal equations, and all other calculations in terms of spherical harmonics, including those of modal excitation coefficients, matrix elements for modal coupling *etc.* (see below). The basic results depend upon the expansion in spherical harmonics of the vector field $\mathbf{s}_k(\mathbf{x})$ and the corresponding perturbation in gravitational potential ϕ_k^1. Following a

traditional approach (e.g. Morse and Feshbach, 1953; Pekeris and Jarosch, 1958) we write:

$$s_r = U(r)Y_l^m(\theta,\phi) \tag{3.48}$$

$$s_\theta = V(r)\partial_\theta Y_l^m(\theta,\phi) + W(r)\partial_\phi Y_l^m(\theta,\phi) \tag{3.49}$$

$$s_\phi = V(r)\text{cosec }\theta\partial_\phi Y_l^m(\theta,\phi) - W(r)\partial_\theta Y_l^m(\theta,\phi) \tag{3.50}$$

$$\phi^1 = P(r)Y_l^m(\theta,\phi) \tag{3.51}$$

where Y_l^m are the spherical harmonics. Here we adopt the fully normalized complex harmonics of Edmonds (1960)

$$Y_l^m(\theta,\phi) = (-1)^m \left[\frac{(2l+1)(l-m)!}{4\pi(l+m)!}\right]^{\frac{1}{2}} P_l^m(\cos\theta)e^{im\phi} \tag{3.52}$$

$$(l = 0,1,2,...;\ m = -l,-l+1,...l)$$

where $P_l^m(x)$ are the associated Legendre functions:

$$P_l^m(x) = \frac{(1-x^2)^{m/2}}{2^l l!}\frac{d^{l+m}}{dx^{l+m}}(x^2-1)^l. \tag{3.53}$$

Y_l^m satisfy the orthogonality relation:

$$\int_{-\pi}^{\pi}\int_0^{\pi} Y_l^{m*}(\theta,\phi)Y_{l'}^{m'}(\theta,\phi)\sin\theta d\theta d\phi = \delta_{ll'}\delta_{mm'}. \tag{3.54}$$

When (3.48 - 3.51) are substituted into the eigenvalue equation (3.34) they give ordinary differential equations for U, V, W, P which are independent of m. These admit two kinds of solution (i) solutions with $U = V = P = 0$, termed *toroidal modes* and (ii) solutions with $W = 0$, termed *spheroidal* or *poloidal modes.* Collectively U, V, W, P are sometimes called the scalar eigenfunctions and those among them which are not identically zero satisfy linear systems of ordinary differential equations, subject to homogeneous boundary conditions. These equations have solutions only for particular, discrete values of ω_k which are the eigenfrequencies of the corresponding free oscillations. By virtue of these results modes may be identified according to *mode type* q (spheroidal or toroidal), *angular order* l, *azimuthal order* m, and *overtone number* n, where the n enumerates the eigenfrequencies, in increasing order, for a given mode type and angular order. The mode index k used earlier may be thought of as consisting of the four subindices $k = (q,l,m,n)$. Since the ordinary differential equations governing the scalar eigenfunctions are independent of m the eigenfrequencies ω_k are the same for all m in the allowed range $-l \le m \le l$; i.e. there are $2l+1$ different eigenfunctions corresponding to the same eigenvalue ω_k which are said, therefore, to be constitute a $(2l+1)$-fold degenerate *multiplet.* Individual members of a multiplet are termed *singlets.* The normal mode multiplets are conventionally referred to by the notations ${}_nS_l$ for spheroidal modes and ${}_nT_l$ for toroidal modes. The spheroidal modes with $l = 0$ have

eigenfunctions which posess only radial displacements and are spherically symmetric. These are termed the *radial modes.*

Having introduced the representation of eigenfunctions in terms of spherical harmonics, it is convenient to write the fundamental equation (3.47) in the simplified form (Woodhouse and Girnius, 1982)

$$\mathbf{u}(\mathbf{x}_r, t) = \sum_k \sum_{m=-l}^{l} S_k^m(\mathbf{x}_s)\mathbf{s}_k^m(\underline{x}_r)e^{i\tilde{\omega}t} \tag{3.55}$$

where the real part is understood. In writing (3.47) in this way we have introduced certain notational changes. First we have redefined the mode index k so that it now refers to *multiplets*: $k = (q, l, n)$; individual singlets within a multiplet are labelled explicitly by the additional index m. Second, we have omitted the the first term in brackets [] in (3.47). This term contributes a time-independent displacement field, which represents the final configuration of the model after all modes have died away. By omitting it, therefore, we obtain an expression representing the displacement field relative to the final, rather than the initial configuration of the model. (In fact the static offset is not observed seismically owing to noise and instrument characteristics.) Third, we have defined the complex frequency

$$\tilde{\omega}_k = \omega_k(1 + i/2Q_k). \tag{3.56}$$

in order that the exponential in (3.55) includes the decaying exponential in (3.47). Fourth, we have defined:

$$S_k^m(\mathbf{x}_s) = -M_{ij}e_{ij}^{(k)*}(\mathbf{x}_s). \tag{3.57}$$

Finally, the location, $\mathbf{x}$, at which the diplacement is evaluated has been given the subsrcript r to emphasize that in comparing with observations the seismogram is evaluated at the receiver location.

A particular seismogram is obtained by operating upon (3.55) with the 'instrument vector' $\mathbf{v}$, which is defined to be a unit vector in the direction of motion sensed by the instrument; $\mathbf{v}$ may also incorporate an operator, or, in the frequency domain a function of frequency, characterizing the instrument response. The seimogram may then be written in a way which involves the source and receiver rather symmetrically:

$$\mathbf{v} \cdot \mathbf{u} = \sum_{km} R_k^m(\theta_r, \phi_r)S_k^m(\theta_s, \phi_s)e^{i\tilde{\omega}_k t} \tag{3.58}$$

where $R_k^m(\theta_r, \phi_r)$, $S_k^m(\theta_s, \phi_s)$ are given by expressions involving spherical harmonics evaluated at the receiver and source. Explictly

$$R_k^m(\theta_r, \phi_r) = \sum_{N=-1}^{1} R_{kN}Y_l^{Nm}(\theta_r, \phi_r) \tag{3.59}$$

$$S_k^m(\theta_s, \phi_s) = \sum_{N=-2}^{2} S_{kN}Y_l^{Nm}(\theta_s, \phi_s) \tag{3.60}$$

where Y_l^{Nm} are the generalized spherical harmonics of Phinney and Burridge (1973) and where $R_{kN} = R_k^N(0,0)$, $S_{kN} = S_k^N(0,0)$ are given by expressions involving the scalar eigenfunctions U, V, W evaluated at the surface and at the source depth, respectively. The formulae for R_{kN} involve the spherical components of the receiver vector v_r, v_θ, v_ϕ and those for S_{kN} involve the moment tensor components M_{rr}, $M_{\theta\theta}$, $M_{\phi\phi}$, $M_{r\theta}$, $M_{r\phi}$, $M_{\theta\phi}$ (see Woodhouse and Girnius, 1982 for explicit formulae).

4 General characteristics of modal multiplets

Normal mode multiplets can be though of as points in the $\omega - l$ plane. Figs 1a., 1b., taken from Gilbert and Dziewonski (1975), show such *dispersion diagrams* for the low frequency toroidal and spheroidal modes. Lines joining the dots define lines of constant overtone number n. By convention the lowest frequency mode, for a given l, is designated the *fundamental mode* and has $n = 0$. These correspond to the fundamental mode Love and Rayleigh waves in the toroidal and spheroidal case, respectively. The solid dots in Fig 1. indicate modes which had been observed up to 1975.

Presently we shall take a tour of the $\omega - l$ plane, showing examples of eigenfunctions, in order to gain some physical insight into the nature of the modes. Before doing this, however, it is useful to introduce the concept of a *differential kernel*, which is a function representing the sensitivity of a modal eigenfrequency to small changes in the (spherically symmetric) earth model. This brings us into the realm of *perturbation theory*. This is of great importance if we whish to make inferences about earth structure from modal measurements. Suppose that a number of modal frequencies ${}_n\omega_l^S$, ${}_n\omega_l^T$ have been measured. These will not agree precisely with the predictions of a given earth model and thus we need to address the question: *How can we modify the earth model to bring it into agreement with the observations?*. This is an *inverse problem* of the type which will be the subject of a number of the lectures at this school. First, however, we need to know how to solve the *forward problem*: *If we make a specified small adjustment to the earth model how will it affect the predictions of the modal eigenfrequencies?*. We do not attempt to cover modal perturbation theory in full detail in these lectures. For the spherical earth, with which we are here concerned, see Backus and Gilbert (1967), Woodhouse (1976). Here we approach the topic in a heuristic way, in order to illustrate some basic principles and to gain insight into the properties of modes and what they are likely to tell us about the Earth.

Suppose that our Earth model consists of a number of spherical layers and, for a given mode, imagine that a particular parameter, density ρ, say, is perturbed by an amount $\delta\rho_i$ in the i-th layer, all other layers remaining unchanged. If the perturbation is small enough, the change in the eigenfrequency of the multiplet will be proportional to $\delta\rho_i$ and so we can define a proportionality constant $K_{\rho i}$ say, such that the corresponding change in the eigenfrequency is given by

$$\delta\omega = K_{\rho i}\frac{\delta\rho_i}{\rho_i^0}\Delta r_i \tag{4.1}$$

where Δr_i is the layer thickness and ρ_i is the unperturbed density in the layer. Then if density is simultaneously perturbed in all layers, and if the perturbations are small enough, the corresponding change in eigenfrequency will be the sum over all layers:

$$\delta\omega = \sum_i K_{\rho i} \frac{\delta\rho_i}{\rho_i} \Delta r_i \tag{4.2}$$

In the limit that the number of layers is infinite this sum will become an integral over radius r and we can write:

$$\delta\omega = \int_0^a K_\rho(r) \frac{\delta\rho(r)}{\rho^0(r)} dr \tag{4.3}$$

$K_\rho(r)$ represents, therefore, the sensitivity of an eigenfrequency to adjustments in density at each radius r. Similarly we can define $K_\mu(r)$, $K_\kappa(r)$ to represent the sensitivity to changes in bulk and shear moduli. Here we shall take ρ, v_P and v_S as the fundamental mechanical parameters of the (isotropic) model, and write:

$$\delta\omega = \int_0^a \left(K_\rho(r) \frac{\delta\rho(r)}{\rho^0(r)} + K_P(r) \frac{\delta v_P(r)}{v_P^0(r)} + K_S(r) \frac{\delta v_S(r)}{v_S^0(r)} \right) dr \tag{4.4}$$

Thus, for each mode, it is possible to define *differential kernels* $K_P(r)$, $K_S(r)$, $K_\rho(r)$ which provide the answer to the forward problem through (4.4). In fact, it is possible to derive exact expressions for such kernels in terms of various quadratic forms involving the scalar eigenfunctons of the mode. Explicit results are given by Backus and Gilbert (1967), Woodhouse (1976), Dziewonski and Anderson (1981).

Figs 2a–e show examples of the eigenfunctions and kernels for a representative set of multiplets. For each multiplet there are two panels, one above the other. The top panel show the scalar eigenfunctions – $\zeta W(r)$ (dashed) for toroidal modes and $U(r)$ (solid) and $\zeta V(r)$ (dashed) for spheroidal modes, where $\zeta^2 = l(l+1)$; the factor ζ is included so that the ratio of the two scalar eigenfunctions for spheroidal modes $U(r)/\zeta V(r)$ correctly reflects the ratio of vertical to horizontal motions. The lower panels for each mode show the differential kernels $K_P(r)$ (solid), $K_S(r)$ (dashed) and $K_\rho(r)$ (dot-dash). The period and Q of the mode are given. All calculations are for the model PREM of Dziewonski and Anderson (1981).

Fig. 2a samples the fundamental toroidal modes. ${}_0T_2$ represents a differential twisting of one hemisphere relative to the other. By examining the eigenfunction we see that the amlitude of the motion is about half as large at the the core-mantle boundary (CMB) as at the surface. In common with all toridal modes, the motion is purely horizontal and does not involve the core. By examining the differential kernels we find that the frequency is increased if v_S is increased anywhere in the mantle, with ρ held fixed, the maximum effect being produced by a (relative) change in v_S close to the 670km discontinuity. If, on the other hand, density is increased, with v_S held fixed, the effect is to reduce the frequency if the change is made in the upper mantle, and to increase it if the change is made in the lower mantle. ${}_0T_5$ has similar properties, except that

its sensitivities are smaller in the lower part of the mantle. Progressing along the fundamental mode branch we see that the modal displacements and sensitivities become concentrated nearer and nearer to the surface, and that sensitivity to density becomes progressively smaller. This is because at high angular order the toroidal modes correspond to Love waves, which may also be thought of as multiply refleced SH waves, having, asymptotically for large l, no sensitivity to density. For example ${}_0T_{80}$, having period 106.7s, has appreciable diplacements only in the upper mantle, and has little sensitivity to v_S at depths greater than 300 km.

Fig. 2b shows examples of toridal mode overtones at fixed angular order $l = 30$. The general property illustrated is that as overtone number increases the eigenfunctions become more oscillatory with depth and penetrate more deeply into the mantle. Also note that for high overtones the density kernel oscillates about zero; although such modes can be affected by localized density perturbations, the effect of smooth density perturbations will be small, since positive and negative contributions will tend to cancel in the integeral (4.4). The v_S kernel, on the other hand, oscillates about a non-zero value; it is this slowly varying mean value which will give the main contribution for smooth changes in $v_S(r)$. Again these properties reflect asymptotic properties of the modes, which may be thought of as standing waves set up by multiply reflecting SH body waves, which dip more steeply into the mantle with increasing overtone number n. Thus, for example, ${}_2T_{30}$ corresponds to SH having a turning point in the lower mantle, whereas ${}_{20}T_{30}$ corresponds to SH waves travelling almost vertically, bouncing between the surface and the CMB (see below).

Fig. 2c samples the fundamental spheroidal modes. ${}_0S_2$, known as the 'football mode', was one of the first observed (Benioff *et al.*, 1961), following the great Chilean earthquake. Its displacements are nonvanishing throughout the Earth; its greatest sensitivity is to perturbations in v_S and, to a lesser extent, ρ in the lowermost mantle and v_P in the upper half of the mantle. Progressing along the fundamental mode branch, displacements and sensitivities become progressively concentrated nearer to the surface, and sensitivity to density diminishes, as in the case of toroidal modes. At higher values of l these modes correspond to Rayleigh waves. Note that their greatest sensitivity is to v_S at a depth somewhat below the surface, which makes them useful for probing upper mantle v_S. On the other hand, they have relatively high sensitivity to v_P at shallow depths.

Fig. 2d shows examples of spheroidal mode overtones, at angular order $l = 30$. These display behaviour similar to, but more complicated than that observed for toroidal mode overtones. Note that the spheroidal mode spectrum contains a variety of different families of modes. For example the (unobserved) mode ${}_3S_{30}$ corresponds to a Stoneley wave propagating at the CMB; this is similar to a Rayleigh wave, but trapped near the CMB rather than near the Earth's surface.

Finally, Fig. 2e shows samples of the radial modes ${}_nS_0$, which, at high n, correspond to vertically travelling $PKIKP$, having little sensitivity to (smooth) density perturbations, almost vanishing sensitivity to v_S, but significant sensitivity to v_P throught the Earth. Note that they have high Q values (i.e. low attenuation), a property which makes

them relatively easy to observe in long seismic records following great earthquakes.

5 Some asymptotic properties of free oscillations

In the foregoing discussion we have mentioned the correspondence between the free oscillation multiplets and various kinds of travelling waves – both body waves and surface waves. The nature of the correspondence between surface waves and modal multiplets has long been apparent, since the traces from which modal spectra can be readily obtained, consist of word-circling Rayleigh and Love wave orbits. The modal peaks appear in the spectrum as a result of the constructive interference which occurs when the spectra of individual wave packets are superposed. The nature of the correspondence between modal overtones and body waves, first pointed out by Brune (1964, 1966), can be made more precise by examining the asymptotic behaviour of solutions of the ordinary differential equations for the scalar eigenfunctions, using the JWKB and related asymptotic techniques (Brodskii, 1975, 1978; Woodhouse, 1978; Kennett and Woodhouse 1978). Here we shall touch only briefly on the topic, since our aim is to gain physical insight into the properties of free oscillations, rather than to develop a complete calculational scheme.

The essential quantitative connection between modes and travelling waves is made by equating the horizontal wavelength (or wavenumber) of the mode with the corresponding horizontal wavelength (or wavenumber) of a travelling wave. For modes, this wavelength is can be derived from the asymptotic properties of the spherical harmonics for large l. Let us consider a source at the pole $\theta = 0$. Such a source excites only the modes having low azimuthal order m. For a point source only the orders having $|m| \leq 2$ are excited (equations 3.59, 3.60).

For fixed m and large l we have (e.g. Abromowitz and Stegun, 1965):

$$Y_l^m(\theta,\phi) \sim \frac{1}{\pi}(\sin\theta)^{-\frac{1}{2}} \cos[(l+\tfrac{1}{2})\theta + \tfrac{1}{2}m\pi - \tfrac{1}{4}\pi]e^{im\phi} \tag{5.1}$$

and, since we are considering a source at the pole, θ plays the role of epicentral distance. Thus we can immediately identify the horizontal wavenumber k ($= 2\pi/\text{wavelength}$) to be

$$k = (l+\tfrac{1}{2})/a. \tag{5.2}$$

The angular order l, therefore, is a proxy for wavenumber k and dispersion diagrams such as those shown in Fig. 1 can be interpreted, for large l, in the same way as are dispersion relations $\omega(k)$ for surface waves. In particular, we can define phase velocity

$$c(\omega) = \frac{\omega}{k} \tag{5.3}$$

and group velocity

$$U(\omega) = \frac{d\omega}{dk} \tag{5.4}$$

In order for these relations to be valid we need to extend the definition of the dispersion curves to continuous, rather than integer values of l. The mathematical justification for doing this is contained in a number of papers on the theory of waves in and around spheres (Watson, 1918; Gilbert 1976). This defines the relationship between the $\omega - l$ plane and the dispersion properties of Love and Rayleigh waves and their overtones.

In the case of body waves we may, similarly, identify the horizontal wavenumber in terms of frequency and *ray parameter* p. From classical ray theory in the spherical Earth, the horizontal wavenumber at the Earth's surface for a monochromatic signal travelling along a ray with given ray parameter $p = dT/d\Delta$ is

$$k = \frac{\omega p}{a}. \tag{5.5}$$

Therefore, using (5.2), we write

$$p = \frac{l + \frac{1}{2}}{\omega} \tag{5.6}$$

Thus a mode of angular order l and angular frequency ω is associated with rays having the ray parameter given by (5.6). For toroidal modes these are S-rays, and for spheroidal modes they are both P- and S-rays. It is well known that rays exist only for ranges of depth for which

$$\frac{r}{v_P(r)} \geq p \qquad \text{for } P\text{-waves} \tag{5.7}$$

$$\frac{r}{v_S(r)} \geq p \qquad \text{for } S\text{-waves} \tag{5.8}$$

In the diagrams of Fig. 2, the ranges of depth for which these inequalities are satisfied are indicated in two columns on the right side of each panel. The left column is for P-waves (relevant only for spheroidal multiplets) and the right column for S waves. Inspecting these figures it will be seen that the sensitivities do have the approximate behaviour we would expect, namely that sensitivity to v_S decays below the S-turning point and that to v_P decays below the P-turning point. In fact there are further quantitative relationships between the dispersion diagrams and the travel times of the corresponding rays, which mean that the information contained in the dispersion diagrams reproduces much of that contained in travel time data.

As an illustration we state the simplest such approximate result (Brune, 1964; Brodskii, 1975), for toroidal modes:

$$\omega = \frac{2\pi(n + \beta)}{\tau(p)} \tag{5.9}$$

where β is either 0 of $\frac{1}{4}$ depending upon whether the S-ray is reflected from the core or turns in the mantle, and where $\tau(p)$ is the ray theoretic *intercept time*

$$\tau(p) = T(p) - p\Delta(p) = 2\int_{r_t(p)}^{a} \left(\frac{1}{v_S^2} - \frac{p^2}{r^2}\right)^{\frac{1}{2}} dr. \tag{5.10}$$

$r_t(p)$ is the turning radius or, in the case that the ray does not have a turning point, the radius of the CMB. Equation (5.9) predicts that along the line of constant $p = (l+\frac{1}{2})/\omega$ in Fig. 1a, the modes are equally spaced, and that their spacing in ω is equal to the ray theoretic quantity $2\pi/\tau(p)$. This result is only approximate, but it reflects the important fact that the information contained in the multiplet frequencies is highly redundant, and duplicates that available from travel times.

6 Oscillations of an aspherical earth model

The calculation of theoretical seismograms in a non-spherical model is difficult and expensive in terms of computer time. Although there exist formulae which are, at least in principle, exact, they involve the manipulation of infinite dimensional matrices and have not been applied in complete form. Similarly, it is conceivable to generate accurate theoretical seismograms by purely numerical techniques (e.g. finite differences), but this has not yet been achieved. In fact the problem encountered in seismic tomography is much greater than that of calculating theoretical seismograms (the forward problem); in order to obtain useful solutions to the inverse problem it will undoubtedly be necessary to carry out calculations equivalent to at least many thousands of forward problems. As a result, several approximate schemes have been developed. Naturally there are intimate connections between the different schemes, which have been ellucidated in a number of theoretical papers. A number of aspects of this complicated field will be described in other lectures at this school. Here I shall only describe some of the schemes which have been applied and indicate some of the connections between them.

Splitting theory. One of the primary effects of asphericity is to remove the degeneracy of the modal spectrum. Each degenerate multiplet is *split* into singlets of slightly different frequency. The theory of modal *splitting* is similar to that governing the splitting of the degenerate energy levels of a spherically symmetric atom subjected to some aspherical perturbing influence, such as a magnetic field. In seismology the theory of splitting has been developed in a series of papers beginning in 1961, when the splitting effect of rotation on the mode ${}_0S_2$ was observed and explained (Backus and Gilbert, 1961; Pekeris et al., 1961; Dahlen, 1968, 1969, 1974; Woodhouse and Dahlen, 1978); see Dahlen (1980) for a review. The way in which asphericity affects a multiplet can be shown to be approximately independent of other multiplets, provided that the multiplet is *isolated* in the spectrum – i.e. not overlapping in frequency with other multiplets. This form of the theory is known as *degenerate splitting theory.* If there are two or more overlapping multiplets which are, nonetheless, an isolated group, a modified version of splitting theory known as *quasi-degenerate splitting theory* can be developed (Dahlen, 1968; Luh, 1973, 1974; Woodhouse 1980; Park, 1987, 1990; Um and Dahlen, 1992), although this form if the theory has not yet been applied to the inverse problem. If all modes are considered to be one group, this theory is essentially exact (Woodhouse, 1983), but it is much too cumbersome to be applied in practice. Thus applications of splitting theory seek to apply a complete theory to a restricted set of

multiplets, judiciously selected to include the effects of interest in a particular class of seismic data (see, for example, Um and Dahlen, 1992).

Consider an isolated multiplet k having, in the spherical Earth, degenerate eigenfunctions $\mathbf{s}_k^m(\mathbf{x})$, $(m = -l, -l+1, ..., l)$ and (complex) eigenfrequency $\tilde{\omega}_k$. Then it possible to define a $(2l+1) \times (2l+1)$ matrix $\mathbf{H}^{(k)}$, known as the splitting matrix of the multiplet, and having elements $H_{mm'}^{(k)}$, which are known linear functionals of the aspherical (and spherical) model perturbations and also include terms due to the rotation and ellipticity of the Earth (for explicit formulae see Woodhouse and Dahlen, 1978). Let $\mathbf{U}^{(k)}$ be the matrix whose columns are the eigenvectors of $\mathbf{H}^{(k)}$ and let $\boldsymbol{\Omega}^{(k)}$ be the corresponding diagonal matrix, whose diagonal elements $\Omega_{ii}^{(k)}$ $(i = 1, 2, ..., 2l+1)$ are the corresponding eigenvalues. Then the result of degenerate splitting is that the eigenfunctions of the aspherical model are given by

$$\mathbf{u}_j^{(k)}(\mathbf{x}) = \sum_m U_{mj}^{(k)} \mathbf{s}_k^m(\mathbf{x}) \qquad (j = 1, 2, ..., 2l+1) \tag{6.1}$$

with corresponding eigenfrequencies $\omega_k + \Omega_{jj}^{(k)}$.

To obtain the perturbed seismogram, it is necessary to expand the equivalent body force density $F(\mathbf{x}, t)$ in terms of $\mathbf{u}_j^{(k)}(\mathbf{x})$. This can be done by making use of the known expansion in terms of $\mathbf{s}_k^m(\mathbf{x})$. It can be shown (Woodhouse and Girnius, 1982) that when this is done one obtains an expression for the perturbed seismogram of the form (c.f. 3.58)

$$\mathbf{v} \cdot \mathbf{u} = \sum_{km} R_k^m(\theta_r, \phi_r) A_k^m(t) e^{i\tilde{\omega}t} \tag{6.2}$$

where $A_k^m(t)$ is the solutions of the initial value problem

$$A_k^m(0) = S_k^m(\theta_s, \phi_s) \tag{6.3}$$

$$\frac{d}{dt} A_k^m(t) = i \sum_{m'} H_{mm'}^{(k)} A_k^{m'}(t) \tag{6.4}$$

Thus at time 0 equations (3.58), for the spherical earth, and (6.2) for the aspherical earth reduce to the same expression, but with increasing time the apparent modal excitations evolve according to (6.4). It is this additional, slow time variation that leads to the split spectrum in the frequency domain. Equation (6.2) leads naturally to an inverse problem for the splitting matrix elements $H_{mm'}^{(k)}$ for the multipet, by seeking to determine the values which enable the spectrum of (6.2) to match observed spectra for the multiplet. This inverse problem can be simplified by noting that the splitting matrix may be represented in terms of rather fewer unknowns c_{st}, which represent the spherical harmonic expansion coefficients of a certain function $\eta^{(k)}(\theta, \phi)$ which is termed the *splitting function* of the multiplet. We have:

$$H_{mm'} = \Omega\beta\delta_{mm'} + \omega_k \sum_{s=0,2,..,2l} \sum_{t=-s}^{s} \gamma_{ls}^{mm't} c_{st} \tag{6.5}$$

$$\eta^{(k)}(\theta, \phi) = \sum_{s=0,2,..,2l} \sum_{t=-s}^{s} c_{st} Y_s^t(\theta, \phi) \tag{6.6}$$

where the first term is the (known) contribution due to the action of Coriolis forces (Dahlen, 1968) and $\gamma_{ls}^{mm't}$ are known numerical coefficients. For further details we refer to Giardini *et al.*, (1987, 1988), Ritzwoller *et al.*, (1988).

The important point is that knowledge of the splitting matrix is equivalent to knowledge of a certain function on the sphere. This function has a finite spherical harmonic expansion, containing only even spherical harmonic degrees. Furthermore the *splitting coefficients* c_{st} are related to the internal heterogeneity of the Earth of degree s and order t by means of differential kernels, in much the same way as was discussed above for the case of spherically symmetric perturbations. Examples of these kernels and the retrieved splitting functions for certain modes, taken from Giardini *et al.* (1988), are shown in Figs. 5 and 6. The kernels depend upon s, but not on t. In fact their dependence on s is small except in the case of very low l modes. In the case that the dependence on s can be neglected, the splitting function $\eta^{(k)}(\theta, \phi)$ is simply a depth average of the *local structure* beneath the point (θ, ϕ), with averaging kernels such as those depicted in Figs. 5,6.

This result reflects the long known fact that within degenerate splitting theory theoretical seismograms have no dependence on odd-degree structure. Since even degree harmonics have even parity under point reflection through the centre of the earth, and odd degree harmonics have odd parity, this means that the the predicted waveforms are sensitive only to the average properties at antipodal points, and have no sensitivity to the difference in structure between antipodal points. Clearly this is not the case for travelling waves, and thus it represents a shortcoming of degenerate splitting theory. Nevertheless it is true for many kinds of data, that the sensitivity to even degree structure is much greater than that for odd degree structure, and consequently that even degree structure is better constrained in tomographic models. Such insensitivity to odd degrees was first pointed out by Backus (1964), in connection with the interpretation of mean phase velocities measured for great circle paths.

Figs. 3, 4, taken from Giardini *et al.*(1988) shows examples of spectral segments which have been used in the inverse problem for c_{st}. Solid lines show observed spectra (amplitude and phase) for narrow intervals in frequency centred on the multiplet of interest. Dashed lines in Figs. 3, 4 show the predictions of splitting theory; in Fig 3 only splitting due to rotation and ellipticity are taken into account, and in Fig. 4 splitting predicted by the retrieved splitting functions has been included. Vertical bars at the bottom of each panel show the distribution of singlets and their relative excitations. These figures illustrate the fact that it is not usually possible to resolve the individual singlet frequencies within the multiplets; this is because of the effects of attenuation and finite record length, which introduce 'smearing' in the spectral domain. The underlying singlets contribute to the spectrum, according to their excitations, but it is only their combined effect which can be observed. It is also clear that the observations and the model predicitions are very discrepant in Fig. 3, which does not include the effects of heterogeneity, but that models of heterogeneity can be found which enable the observations and the theory to be brought into close agreement. Naturally, it is necessary to use many spectra for the same multiplet in order to retrieve the splitting

function of the multiplet. Each observed spectrum yields a different sample of the underlying singlet distribution, counteracting the difficulty of not being able to retrieve the singlet distribution directly.

The strength of this approach is that it enables us to extract information from very long period data which cannot be interpreted in terms of rays and travel times. Since the wavelengths involved are comparable to the Earth's radius, such data average over large volumes of the Earth, enabling us to constrain the very low wavenumbers of the spectrum of heterogeneity. When applied to modes sampling the the Earth's inner core the method confirmed the existence of a strong zonal effect (Masters and Gilbert, 1981; Ritzwoller *et al.*, 1986) and led to its interpretation in terms of inner core anisotropy (Woodhouse *et al.*, 1986; Morelli *et al.*, 1986; Giardini *et al.*, 1987). As illustrated in Fig. 5., there are a number of modes which are ideally suited to estimating mean lower mantle S-heterogeneity (of low degree), and others (Fig. 6) posessing significant sensitivity to mantle v_P. Such information was used by Li *et al.*, to estimate the mean lower mantle ratio of S to P heterogeneity, obtaining a value of $d\ln v_S/d\ln v_P$ much higher than had been anticipated. Some more recent measurements of modal splitting are by Widmer *et al.*, (1992).

The short time approximation. For sufficiently small times, t, equation (6.4) has the solution

$$A_k^m(t) = S_k^m(\theta_s,\phi_s) + it\sum_{m'} H_{mm'}^{(k)} A_k^{m'}(t). \tag{6.7}$$

Since $H_{mm'}^{(k)}$ is linear in the model perturbations, this leads to a linearized relationship between heterogeneity and the seismogram; that is to say it yields the partial derivative of the seismogram with respect to aspherical model perturbations. Using (6.7) in (6.2) we obtain the *short time approximation*

$$\mathbf{v}\cdot\mathbf{u} = \sum_{km} R_k^m(\theta_r,\phi_r) S_k^m(\theta_s,\phi_s)(1+i\lambda_k t)\, e^{i\tilde{\omega}_k t} \tag{6.8}$$

where

$$\lambda_k = \frac{\sum_{mm'} R_k^m(\theta_r,\phi_r) H_{mm'}^{(k)} S_k^{m'}(\theta_s,\phi_s)}{\sum_m R_k^m(\theta_r,\phi_r) S_k^m(\theta_s,\phi_s)}. \tag{6.9}$$

Equation (6.8) can also be written, to the same formal precision,

$$\mathbf{v}\cdot\mathbf{u} = \sum_{km} R_k^m(\theta_r,\phi_r) S_k^m(\theta_s,\phi_s) \exp\{i(\tilde{\omega}_k+\lambda_k)t\}. \tag{6.10}$$

This form of the equation shows that the effect of heterogeneity is to modify the apparent frequency the mode by the amount λ_k which, importantly, depends upon upon the source and receiver locations.

Early observations of the effects of heterogeneity on the measured frequencies of the fundamental mode had identified this effect (Buland *et al.*, 1979). Within the

modal picture it is, at first, puzzling, since one thinks of the eigenfrequencies as purely functions of Earth structure, and not of the path. However, within the travelling wave picture, it is clear that measured phase delays will characterize the path along which surface wave packets propagate between source and receiver. Equations (6.10) provides one of the connections between the mode and ray pictures of the oscillations. The way in which it comes about that the measurement of the location of a spectral peak is affected by the path is illustrated in Fig. 4. For example, Fig. 4d, for the fundamental mode ${}_0S_7$ the peak is moved to the left, since the exitation of the higher frequency singlets is very small, reflecting the fact that the source-receiver great circle path, in this case, samples regions of low phase velocity.

It is of interest to investigate this effect further, and to determine the way in which the location parameter λ_k depends upon the geographical distribution of heterogeneity, as represented by of the splitting function $\eta^{(k)}(\theta,\phi)$. We find

$$\lambda_k = \int_{-\pi}^{\pi}\int_{0}^{\pi} K^{(k)}(\theta,\phi)\eta^{(k)}(\theta,\phi)\sin\theta d\theta d\phi. \tag{6.11}$$

Explicit expressions for the sampling kernel $K^{(k)}(\theta,\phi)$ are given by Woodhouse and Girnius (1982). Figs. 7a,b, taken from their paper, show examples of the these. The figures show a rectangular (linear) projection of the globe and the shape of the kernel is illustrated for a source on the 'equator' at the 'eastmost' (left) end of the plot. The receiver is also on the 'equator', 108° to the 'west'. The kernels are shown (for an explosive source and a vertical instrument) for the fundamental modes ${}_0S_12$ and ${}_0S45$. For both modes the systematic peak along the great circle path is aparrent, becoming more clearly defined as angular order increases. In the limit of large l, λ_k represents just the great-circle average of $\eta^{(k)}$, which, again for large l is equal to the change in eigenfrequency corresponding to the *local* radial structure at each point of the globe. Thus we have:

$$\lambda_k = \frac{1}{2\pi}\int_{\text{great circle}} \delta\omega_{\text{local}}(\theta,\phi)d\sigma \tag{6.12}$$

where $d\sigma$ represents angular distance along the great circle path, a result derived by Jordan (1978) by an asymptotic analysis of the equations governing degenerate splitting. This result is most easily understood in terms of the ray picture of surface wave propagation, where it represents the fact that the phase delay of a surface wave is an integral of local phase slowness along the path (see below). The location parameter λ_k, representing the spectral peak shift, arises from demanding constructive interference of globe-circling wave packets.

The short time approximation (6.7) has been extended to include interactions between all multiplets by Woodhouse (1983) (also Tanimoto, 1984). The resulting formulae can be regarded as giving exact expressions for the partial derivative of a seismogram with respect to perturbations in earth structure from an initial, spherically symmetric, model. Thus, to the extent that seismograms depend linearly on structural perturbations this is all that is needed. Unfortuntely, such dependence is far from linear

whenever the perturbations result in travel time shifts more that a fraction of the period. The situation can be alleviated somewhat by incorporating the secular terms (i.e. those proportional to t) into frequency adjustments such as was done in passing from (6.8) to (6.10). The resulting expression for the seimogram can be written

$$\mathbf{v} \cdot \mathbf{u} = \sum_k A_k \exp\left\{i\overline{\omega}_k t\right\}. \tag{6.13}$$

with (neglecting density perturbations which introduce additional terms)

$$\overline{\omega}_k^2 = \omega_k^2 + \frac{\sum_{mm'} R_k^m H_{mm'}^{kk} S_k^{m'}}{\sum_m R_k^m S_k^m} \tag{6.14}$$

$$A_k = \sum_m R_k^m S_k^m + \sum_{k \neq k'} \frac{1}{\omega_k^2 - \omega_{k'}^2} \left\{ \sum_{mm'} R_k^m H_{mm'}^{kk'} S_{k'}^{m'} + \sum_{mm'} R_{k'}^{m'} H_{m'm}^{k'k} S_k^m \right\}. \tag{6.15}$$

Where the *matrix elements* $H_{mm'}^{kk'}$ are defined in a similar way to the splitting matrix elements $H_{mm'}^{(k)}$ introduced above, but which now are defined for all *pairs* of multiplets. The *self coupling* terms are (again neglecting density perturbations) $H_{mm'}^{kk} = 2\omega_k H_{mm'}^{(k)}$.

Certain alternative exact and asymptotic approximations to these expressions have been derived, which enable further connections to be made between the mode and ray pictures (Romanowicz and Roult, 1986, 1988; Romanowicz, 1987; Snieder and Romanowicz, 1988; Romanowicz and Snieder, 1988) and which also ellucidate the connection with the Born approximation and incorporate the effects of anisotropy. First order scattering theory, which leads to the Born approximation, is an alternative way of calulating the linearized effect of heterogeneity, which must, of course, coincide with the theory outlined here. In addition, the connections between the mode and ray pictures point towards the shortcomings of ray theory and enable the 'width' of a ray to be quantified, in much the same way as it was shown above that the location parameter λ_k is characterized by a distributed averaging kernel over the globe, rather than by a simple line average around the great circle. Li and Tanimoto (1993) derive a practicable algorithm for calculating the differential kernels of long period body waves by limiting the summations in (6.15) to those in the group velocity window close to $\Delta/T(\Delta)$, where Δ and $T(\Delta)$ are the distance and travel time of the phase of interest. Li and Romanowicz, (1994) apply this method to the inversion of three dimensional mantle structure and compare the results with those obtained using a less sophisticated theory. Certain higher order scattering approximations have also been developed (e.g. Pollitz, 1994). A number of such developments will be discussed in other lectures at this school.

These developments are adding to our understanding of the way in which heterogeneity affects seismic observations; it must be borne in mind, however, that results of this kind depend upon the short time approximation, and while they enable the connections between the ray and mode pictures to be clarified, they do not supercede ray theory itself. Ray theory is an asymptotic theory which depends upon the assumption that the scale lengths characterizing heterogeneity are large compared with the

wavelengths of interest. It is not a short-time theory, and is not a perturbation theory, in that it can deal with arbitrarly large structural variations, provided that they are sufficiently smooth on the scale of a wavelength. Thus the domains of applicability of ray theory and scattering theory are different. Naturally, where their domains of applicability intersect, they give similar results, and the linearized predicitions of ray theory must agree, in the case of sufficiently smooth perturbations, with the predictions of first order scattering theory.

Surface wave ray theory The fundamental idea of ray theory is that *locally* any kind of wave, of fixed frequency ω, is approximated by plane wave of the form

$$u = A\exp(i\omega t - ikx) \tag{6.16}$$

Since we are here considering surface waves, x is a measure of distance in some direction (the direction of propagation) in the surface, and u is some component of displacement. Since the surface may be curved, and since the properties of the medium vary laterally we need to allow the horizontal wavenumber k and the amplitude A to vary laterally on the scale of variation of the medium. A general way of doing this (Bretherton, 1968; Gjevik, 1973; Woodhouse, 1974; Woodhouse and Wong, 1986) is to replace (6.16) by the expression

$$\mathbf{u}(\mathbf{x},r,t) = \mathbf{A}(\mathbf{x},r,t)\exp(-i\psi(\mathbf{x},t)) \tag{6.17}$$

and to *define* the local wavenumber and frequency of the wave to be

$$k_\sigma = \frac{\partial\psi}{\partial x^\sigma}, \qquad \omega = -\frac{\partial\psi}{\partial t} \tag{6.18}$$

Here $\mathbf{x}$ denotes a pair of coordinates in the surface, which we denote individually by x^σ ($\sigma = 1,2$), $x^1 = \theta$, $x^2 = \phi$, say. We then demand (in a mathematically well defined way) that the amplitude $\mathbf{A}$ and the wavenumber k (and possibly the frequency ω) vary *slowly* – on the same scale as the lateral variations in structure. It can then be shown that $\mathbf{A}(\mathbf{x},r,t)$, as a function of r at constant x_σ, t, must be an eigenfunction of the *local* eigenvalue problem corresponding to the frequency and wavenumber ω, k_σ – i.e. its dependence on r must be the same as in a laterally homogeneous medium having everywere the properties which exist at the point x_σ, t. Of course, although it is allowed by the theory we shall only need to consider the case in which the structure is independent of t. As a consequence, frequency and wavenumber must be related by the local dispersion relation, $\omega = \omega(k_\sigma, x_\sigma)$ i.e.

$$\frac{\partial\psi}{\partial t} + \omega\left(\frac{\partial\psi}{\partial x_\sigma}, x^\sigma\right) = 0. \tag{6.19}$$

This is a partial differetial equation for the phase ψ, and it is in the form of the *Hamilton-Jacobi equation* which occurs in classical mechanics. The dispersion relation $\omega(k_\sigma, x_\sigma)$ plays exactly the role that is played by the Hamiltonian $H(p_\sigma, q_\sigma)$, where p_σ, q_σ are the canonical momenta and coordinates of a mechanical system (see e.g. Goldstein, 1959).

The solution of this system is obtained by applying the *method of characteristics* which yield Hamilton's canonical equations,

$$\dot{x^\sigma} = \frac{\partial \omega}{\partial k_\sigma} \tag{6.20}$$

$$\dot{k_\sigma} = -\frac{\partial \omega}{\partial x_\sigma} \tag{6.21}$$

where '˙' denotes the time derivative along the characteristic curve. The phase function ψ is to be obtained by integrating along the characteristic:

$$\psi = \int (\omega - k_\sigma \dot{x}^\sigma)\, dt \qquad \text{(summation assumed)} \tag{6.22}$$

Since the Hamiltonian $\omega(k_\sigma, x^\sigma)$ has no explicit dependence on t it is a 'constant of the motion'; that is to say, solutions of (6.20) will be such that $\omega(k_\sigma, x^\sigma)$ is constant. Consequently we have

$$\psi = \omega t - \int (k_\sigma \dot{x}^\sigma)\, dt \tag{6.23}$$

The canonical equations constitute the *ray tracing equations* for surface waves of a given constant frequency. Of course, the equations depend upon frequency, and so the ray trajectories will depend upon the frequency. Notice that, in general, the wave vector k_σ is not necessarily parallel to the ray, although it will be in the case that the dispersion relation is transversly isotropic. The ray represents the transport of energy at the group velocity

$$U = \left(g_{\sigma\nu} \frac{\partial \omega}{\partial k_\sigma} \frac{\partial \omega}{\partial k_\nu} \right)^{\frac{1}{2}} \tag{6.24}$$

where $g_{\sigma\nu}$ is the covariant metric tensor in the surface. In the case of a sphere of radius a

$$g_{11} = a^2, \qquad g_{22} = a^2 \sin^2\theta, \qquad g_{12} = g_{21} = 0. \tag{6.25}$$

The usual spherical components or the wave vector are

$$k_\theta = k_1/a, \qquad k_\phi = \text{cosec}\ \theta k_2/a \tag{6.26}$$

and those of the ray tangent ν, say, are

$$\nu_\theta = a\dot{\theta}/U; \qquad \nu_\phi = a \sin\theta \dot{\phi}/U. \tag{6.27}$$

As in the ray theory for body waves, it can be shown that there is an inverse relationship between between the square of the wave amplitude and the spreading of neighbouring rays, by virtue of the fact that, in the absence of attenuation, energy is conserved within the ray tube. This relationship takes the form

$$U(\omega, x_\sigma) \int_0^a \rho |\mathbf{A}(\mathbf{x}, r, t)|^2 dr \times \text{(ray tube width)} = \text{constant along the ray} \quad (6.28)$$

and since all other attributes of $\mathbf{A}(\mathbf{x}, r, t)$ are determined by the fact that it is a local eigenfunction, this equation determines the variation of wave amplitude along the ray.

While the foregoing theory is general, we shall now specialize to the case that the dispersion relation is isotropic. The case of azimuthal anisotropy will be discussed further in other lectures at this school. We write

$$\omega = \omega(k, x_\sigma) \quad (6.29)$$

where

$$k = (g^{\sigma\nu} k_\sigma k_\nu)^{\frac{1}{2}} = (k_\theta^2 + k_\phi^2)^{\frac{1}{2}} \quad (6.30)$$

The ray tracing equations can, in this case be recast in terms of the phase velocity, at constant frequency ω as a function of position: $c(\omega, x_\sigma) = \omega/k$. Taking ϕ to be the independent variable and $\gamma = \cot\theta$ to be the dependent variable, the ray trajectory $\gamma(\phi)$ satisfies the second order ordinary differential equation (Woodhouse and Wong, 1986):

$$\frac{d^2\gamma}{d\phi r} + \gamma = \left\{ \sin^2\theta \left(\frac{d\gamma}{d\phi} \right)^2 + 1 \right\} \left(\partial_\theta + \frac{d\gamma}{d\phi} \partial_\phi \right) \ln c(\omega, \theta, \phi). \quad (6.31)$$

Ray tracing equations equivalent to this were derived by Jobert and Jobert (1983). This is an exact ray tracing equation, but it is particularly useful for investigating the behaviour of rays in the case of slight heterogeneity, in which case the right side is a first order quantity, and first order approximations to the ray trajectory and other ray properties can be easily obtained by substituting the unperturbed ray trajectory, namely the great circle

$$\gamma(\phi) = (\text{const.}) \times \sin(\phi - \phi_0) \quad (6.32)$$

into the the right hand side, and making use of the well known solutions, in terms of integrals, of the inhomogeneous simple harmonic equation. This can made particularly simple if the coordinate system is chosen in such a way that the unperturbed ray lies along the 'equator', in which case the equation of the unperturbed ray is simply $\gamma(\phi) = 0$.

Using this approach Woodhouse and Wong (1986) have derived approximate formulae for the phase, amplitude and off-azimuth arrival direction. For high orbits such linearized results from ray theory are often poor approximations to the results of exact ray calculations (for realistic low order models of heterogeneity); however they lend some insight into the magnitude and character of the effect of heterogeneity on surface waves. In particular, they allow us to write down simple formulae for the phase and amplitude anomalies to be found in successive orbits observed at the same station. These can be written in terms of the orbit number n of odd (R_1, R_3 ..., G_1, G_3, etc.)

and even (R_2, R_4 ..., G_2, G_4, etc.) orbits of surface waves. For phase anomaly $\delta\psi$ and amplitude anomaly $\delta \ln A$ these results can be written:

$$\delta\psi = -\frac{\omega a}{c(\omega)}[I_1 + \tfrac{1}{2}(n-1)I_2] \qquad (n \text{ odd}) \tag{6.33}$$

$$\delta\psi = -\frac{\omega a}{c(\omega)}[-I_1 + \tfrac{1}{2}nI_2] \qquad (n \text{ even}) \tag{6.34}$$

$$\delta \ln A = \tfrac{1}{2}\text{cosec } \Delta[J_1 + \tfrac{1}{2}(n-1)J_2] \qquad (n \text{ odd}) \tag{6.35}$$

$$\delta \ln A = \tfrac{1}{2}\text{cosec } \Delta[J_1 - \tfrac{1}{2}nJ_2] \qquad (n \text{ even}) \tag{6.36}$$

(6.37)

where I_1, I_2 (and similarly J_1, J_2) are certain integrals taken over the minor arc and great circle path respectively. These integrals are:

$$I = \int \delta(\ln c)d\phi \tag{6.38}$$

$$J = \int \sin(\Delta - \phi)[\sin\phi\partial_\theta^2 - \cos\phi\partial_\phi]\delta(\ln c)d\phi \tag{6.39}$$

assuming that the coordinates are such that the receiver on the 'equator' at $(\theta, \phi) = (\pi/2, 0)$ and the receiver is at $(\pi/2, \Delta)$. Equations (6.35), (6.36) neglect the effect due to the fact that the surface amplitude of the normalized eigenfunction (i.e. normalized to unit energy surface density) depends upon local structure. The results (6.33), (6.34) are simply a representation of Fermat's principle – that the phase perturbation, to first order in the heterogneity, is the intergral of the perturbation in phase slowness ($\delta[1/c]$) with respect to distance travelled along the ray. The formulae (6.33),(6.34) illustrate the well known fact that, assuming Fermat's principle to hold, multiply orbiting mantle waves accumulate the the same phase anomaly for each great circle passage. The corresponding prediction for amplitude anomalies is that orbits of one sense are amplified by the same factor for each great circle passage, and that orbits of the oposite sense are deamplified by the same factor, a phenomenon frequently observed in the data, demonstrating the importance of the focusing effect.

Examples of measured amplitude anomalies, together with exact and linearized (ray theoretic) model calculations are shown in Figs. 8,9, taken from Woodhouse and Wong (1986). The ray paths traced using exact ray theory are also shown, in a projection for which the source is on the 'equator' at zero 'longitude' and the great circle path lies along the 'equator'. Fig 8. shows an example for which the paths are not greatly deviated from the great circle, and for which the observations and the two theoretical results show some measure of agreement. Fig. 9 shows an example where the paths deviate by large amounts from the great circle and for which the data are in better agreement with the exact ray theoretic results, which deviate greatly from linearized ray theory. These results show that there are very large amplitude effects, both observed and predicted, due to focusing and defocusing of the ray bundle. These significantly complicate the problem of estimating the attenuation of mantle waves.

Wong (1989) addressed the nonlinear inverse problem of using both phase and amplitude of mantle waves to determine phase velocity distributions for Love and Rayleigh waves in the period range 150–350s, up to spherical harmonic degree and order 12. This involves iteratively updating the model and the ray paths until convergence is achieved. While excellent results were obtained for phase (more than 70% variance reduction for all but the longest periods), the variance reduction in amplitudes was only of order 20%. This probably indicates that degrees higher than 12 have an important influence on amplitudes.

The connection of the results of ray theory, e.g. (6.33)–(6.36), with those derived from the modal approach can be made by recognizing that

$$\frac{\delta\omega_{\text{local}}}{\omega} = \frac{U}{c}\frac{\delta c}{c} \tag{6.40}$$

This form arises from the fact the $\delta\omega_{\text{local}}$ is defined as the local perturbation in eigenfrequency at constant k (or constant l), whereas δc is the phase velocity perturbation at constant ω. Using these relationships (or from first principles) it can be shown (Woodhouse and Dziewonski, 1984) that the phase perturbations (6.33), (6.34), at the orbital group arrival times, can be mimicked by a calculating the contribution to the seismogram as in a spherical model, but with an adjustment δ_θ (which is different for different multiplets) to the arc distance, together with an adjustment to the modal eigenfrequency $\widehat{\delta\omega}$. We find

$$\delta\psi = ak\delta\theta - \widehat{\delta\omega}t \qquad (n \text{ odd}) \tag{6.41}$$

$$\delta\psi = -ak\delta\theta - \widehat{\delta\omega}t \qquad (n \text{ even}) \tag{6.42}$$

where t is the group arrival time of the given orbit

$$t = a(\Delta + (n-1)\pi)/U \qquad (n \text{ odd}) \tag{6.43}$$

$$t = a(-\Delta + n\pi)/U \qquad (n \text{ even}) \tag{6.44}$$

$$\tag{6.45}$$

and where

$$\delta\theta = \frac{\Delta}{kU}(\widehat{\delta\omega} - \widetilde{\delta\omega}) \tag{6.46}$$

The quantities $\widehat{\delta\omega}$, $\widetilde{\delta\omega}$ are defined to be the great circle average and the minor arc average, respectively, of $\delta\omega_{\text{local}}$. This provides an alternative derivation of the formula (6.12) of Jordan (1978) for the observed frequency shift for a given path. Additionally, it gives a simple way of calculating seismograms which incorporate the effects of phase delays along incomplete arcs. It has been shown by Romanowicz (1987) that the this result, together with the amplitude effects predicted by (6.35), (6.36) can be obtained by an asymptotic analysis of the scattering approximation (6.13), when coupling between neighbouring modes along the same branch is taken into account. This simplified version of ray theory, which incorporates only an approximation to the ray theoretic prediction

of the phase, is a very useful one for waveform inversion, and has been applied, in many studies (e.g. Woodhouse and Dziewonski, 1984, 1986, 1989; Tanimoto, 1987, 1988, 1990; Su and Dziewonski, 1991; Su *et al.*1994) to both surface wave and long period body wave data. Its shortcoming is that it is not very accurate for direct body wave phases, since it predicts that the observed seismogram depends only upon the horizontally averaged structure, which is clearly not a good approximation in many cases. It is a good approximation (within the the limitations of ray theory) for the fundamental mode and the low overtones, which constitute a major part of the long period body wave signal. Its limitations have recently been investigated by Li and Romanowicz (1994).

In the spectral domain, the measurent of frequency shifts in individual spectra for the fundamental modes, has been extensively applied to constrain even degree mantle structure (e.g. Masters *et al.*1982; Smith and Masters, 1989); the related and traditional techniqe of measuring phase and group delays over numerous paths was also among the earliest to ellucidate clear patterns of heterogeneity in the mantle (e.g. Nakanishi and Anderson, 1982, 1983, 1984; Nataf *et al.*1984, 1986).

References

Abromowitz, M. and I. A. Stegun, *Handbook of Mathematical Functions*, Dover Publications, New York, 1965.

Backus, G. E., Geographical interpretation of measurements of average phase velocities of surface waves over great circular and great semi-circular paths, *Bull. Seism. Soc. Am.*, **54**, 571-610, 1964.

Backus, G. E. and J. F. Gilbert, The rotational splitting of the free oscillations of the Earth, *Proc. Nat. Acad. Sci.*, **47**, 362-371, 1961.

Backus, G. E. and F. Gilbert, Numerical applications of a formalism for geophysical inverse problems, *Geophys. J. R. Astron. Soc.*, **13**, 247-276, 1967.

Backus, G. E. and M. Mulcahy, Moment tensors and other phenomenological descriptions of sesimic sources, I. Continuous displacements, *Geophys. J. R. Astron. Soc.*, **46**, 341-362, 1976.

Benioff, H., F. Press and S. W. Smith, Excitation of the free oscillations of the Earth by earthquakes, *J. Geophys. Res.*, **66**, 605-619, 1961.

Biot, M. A., *Mechanics of Incremental Deformations*, John Wiley, New York, 504pp, 1965.

Bretherton, F. P., Propagation in slowly varying waveguides, *Proc. R. Soc. Lond.*, **A302**, 555, 1968.

Brodskii, M. A., On an application of asymptotic methods for the inverse problem of toroidal oscillations, *Comput. Seismol.*, **8**, 162-174 (in Russian), 1975.

Brodskii, M. A., An asymptotic method of investigation of rays and inversion fro spheroidal oscillations of an elastic sphere, *Comput. Seismol.*, **10**, 150-168 (in Russian), 1978.

Brune, J. N., Travel times, body waves and normal modes of the Earth, *Bull. Seism. Soc. Am.*, **54**, 2099-2128, 1964.

Brune, J. N., P and S wave travel times and spheroidal normal modes of a homogeneous sphere, *J. Geophys. Res.*, **71**, 2959-2965, 1966.

Buland, R., J. Berger and F. Gilbert, Observations from the IDA network of attenuation and splitting during a recent earthquake, *Nature*, **277**, 358-362, 1979.

Dahlen, F. A., The normal modes of a rotating, elliptical earth, *Geophys J. R. Astron. Soc.*, **16**, 329-367, 1968.

Dahlen, F. A., The normal modes of a rotating, elliptical earth, II, Near resonant multiplet coupling, *Geophys. J. R. Astron. Soc.*, **18**, 397-436, 1969.

Dahlen, F. A., Elastic dislocation theory for a self-gravitating elastic configuration with an initial static stress field, *Geophys. J. R. astr. Soc.*, **28**, 357-383, 1972.

Dahlen, F. A., Elastic dislocation theory for a self-gravitating elsatic cinfiguration with an initial static stress field. II. Energy release, *Geophys. J. R. astr. Soc.*, **31**, 469-484, 1973.

Dahlen, F. A., Inference of the lateral heterogeneity of the Earth from eigenfrequency spectrum: a linear inverse problem, *Geophys. J. R. Astron. Soc.*, **38**, 143-167, 1974.

Dahlen, F. A., Splitting of the free oscillations of the Earth, in: *Physics of the Earth's Interior* (A. M. Dziewonski and E. Bosci, eds.), *Proc. "Enrico Fermi" Int. Sch. Phys.*, **78**, 82-126, 1980.

Dahlen, F. A. and M. L. Smith, The influence of rotation on the free oscillations of the Earth, *Philos. Trans. R. Soc. Lond., Ser. A*, **279**, 583-629, 1975.

Dziewonski, A. M. and D. L. Anderson, Preliminary Reference Earth Model, *Phys. Earth Planet. Int.*, **25**, 297-356, 1981.

Dziewonski, A. M. and J. H. Woodhouse, Studies of the seismic source using normal mode theory, *Proc. Enrico Fermi Sch. Phys.*, **85** (H. Kanamori and E. Boschi, eds.), 45-137, 1983.

Dziewonski, A. M. and D. L. Anderson, Preliminary Reference Earth Model, *Phys. Earth Planet. Int.*, **25**, 297-356, 1981.

Edmonds, A. R., *Angular Momentum and Quantum Mechanics*, Princeton University Press, Princeton, NJ, 1960.

Geller, R. J., Elastodynamics in a laterally heterogeneous, self-gravitating body, *Geophys. J. R. astr. Soc.*, **94**, 271-283, 1988.

Giardini, D., X. Li and J. H. Woodhouse, Three dimensional structure of the Earth from splitting in free oscillation spectra, *Nature*, **325**, 405-411, 1987.

Giardini, D., X.-D. Li and J. H. Woodhouse, Splitting functions of long period normal modes of the Earth, *J. Geophys. Res.*, **93**, 13716-13742, 1988.

Gilbert, F., Excitation of normal modes of the Earth by earthquake sources, *Geophys. J. R. Astron. Soc.*, **22**, 223-226, 1971.

Gilbert, F., The representation of seismic displacements in terms of travelling waves, *Geophys. J. R. Astron. Soc.*, **44**, 275-280, 1976.

Gilbert, F. and A. M. Dziewonski, An application of normal mode theory to the retrieval of structural parameters and source mechanisms from seismic spectra, *Philos. Trans. R. Soc. Lond. A*, **278**, 187-269, 1975.

Gjevik, B., A variational method for Love waves in nonhorizontally layered structures, *Bull. Seism. Soc. Am.*, **63**, 1013, 1973.

Goldstein, H. *Classical Mechanics*, Addison-Wesley, 399pp., 1959.

Jobert, N. and G. Jobert, An application of ray theory to the propagation of waves along a laterally heterogeneous spherical surface, *Geophys. Res. Lett.*, **10**, 1148-1151, 1983.

Jordan, T. H., A procedure for estimating lateral variations from low-frequency eigenspectra data, *Geophys. J. R. Astron. Soc.*, **52**, 441-455, 1978.

Kennett, B. L. N. and J. H. Woodhouse, On high-frequency spheroidal modes and the structure of the upper mantle, *Geophys. J. R. Astron. Soc.*, **55**, 333-350, 1978.

Li, X.-D. and T. Tanimoto, Waveforms of long-period body waves in a slightly aspherical earth model, *Geophys. J. Int.*, **112**, 92-102, 1993.

Li, X.-D. and B. Romanowicz, Comparison of global waveform inversion with and without considering cross-branc coupling, *Geophys. J. Int.*, submitted, 1994.

Love, A. E. H., *Some Problems in Geodynamics*, Cambridge University Press, 1911.

Luh, P. C., Free oscillations of the laterally inhomogeneous Earth: Quasi-degenerate multiplet coupling, *Geophys. J. R. Astron. Soc.*, **32**, 187-202, 1973.

Luh, P. C., Normal modes of a rotating, self gravitating inhomogeneous Earth, *Geophys. J. R. Astron. Soc.*, **38**, 187-224, 1974.

Malvern, L. E., *Introduction to the mechanics of a continuous medium*, Prentice-Hall, Englewood Cliffs, New Jersey, 1969.

Masters, G. and F. Gilbert, Structure of the inner core inferred from observations of its spheroidal shear modes, *Geophys. Res. Lett.*, **8**, 569-571, 1981.

Masters, G., T. H. Jordan, P. G. Silver and F. Gilbert, Aspherical earth structure from fundamental spheroidal mode data, *Nature*, **298**, 609-613, 1982.

Morelli, A., A. M. Dziewonski and J. H. Woodhouse, Anisotropy of the inner core inferred from PKIKP travel times, *Geophys. Res. Lett.*, **13**, 1545-1548, 1986.

Morse, P. M. and H. Feshbach, *Methods of Theoretical Physics*, McGraw Hill, 1953.

Nakanishi, I. and D. L. Anderson, Worldwide distribution of group velocity of mantle Rayleigh waves as determined by spherical harmonic inversion, *Bull. Seism. Soc. Am.*, **72**, 1185-1194, 1982.

Nakanishi, I. and D. L. Anderson, Measurement of mantle wave velocities and inversion for lateral heterogeneity and anisotropy, I. Analysis of great circle phase velocities, *J. Geophys. Res.*, **88**, 10267-10283, 1983.

Nakanishi, I. and D. L. Anderson, Measurement of mantle wave velocities and inversion for lateral heterogeneity and anisotropy, II. Analysis by the single station method, *Geophys. J. R. Astron. Soc.*, **78**, 573-618, 1984.

Nataf, H.-C., I. Nakanishi and D. L. Anderson, Anisotropy and shear velocity heterogeneities in the upper mantle, *Geophys. Res. Lett.*, **11**, 109-112, 1984.

Nataf, H.-C., I. Nakanishi and D. L. Anderson, Measurement of mantle wave velocities and inversion for lateral heterogeneity and anisotropy, III. Inversion, *J. Geophys. Res.*, **91**, 7261-7307, 1986.

Park, J., Asymptotic coupled-mode expressions for multiplet amplitude anomalies and frequency shifts on an aspherical Earth, *Geophys. J. R. Astron. Soc.*, **90**, 129-169, 1987.

Park, J., Free oscillation coupling theory, in: *Mathematical Geophysics* (N. J. Vlaar, G. Nolet, M. J. R. Wortel and S. A. P. L. Cloetingh, eds.), D. Reidel, 31-52, 1988.

Park, J., The subspace projection method for constructing coupled-mode synthetic seismograms, *Geophys. J. Int.*, **101**, 111-123, 1990.

Pekeris, C. L. and H. Jarosch, The free oscillations of the Earth, *Contributions in Geophysics in Honor of Beno Gutenberg*, pp171-192, Pergamon, New York, 1958.

Pekeris, C. L., A. Alterman and H. Jarosch, Rotational multiplets in the spectrum of the Earth, *Phys. Rev.*, **122**, 1692-1700, 1961.

Phinney, R. A. and R. Burridge, Representation of the elastic-gravitational excitation of a spherical earth model by generalized spherical harmonics, *Geophys. J. R. Astron. Soc.*, **34**, 451-487, 1973.

Pollitz, F. F, Surface wave scattering from sharp latteral discontinuities *J. Geophys. Res.*, in press, 1994.

Ritzwoller, M., G. Masters and F. Gilbert, Observations of anomalous splitting and their interpretation in terms of aspherical structure, *J. Geophys. Res.*, **91**, 10203-10228, 1986.

Ritzwoller, M., G. Masters and F. Gilbert, Constraining aspherical structure with low frequency interaction coefficients: Application to uncoupled multiplets, *J. Geophys. Res.*, **93**, 6369-6396, 1988.

Romanowicz, B., Multiplet-multiplet coupling due to lateral heterogeneity: asymptotic effects on the amplitude and frequency of the Earth's normal modes, *Geophys. J. R. Astron. Soc.*, **90**, 75-100, 1987.

Romanowicz, B. and G. Roult, First-order asymptotics for the eigenfrequencies of the Earth and application to the retrieval of large-scale lateral variations of structure, *Geophys. J. R. Astron. Soc.*, **87**, 209-239, 1986.

Romanowicz, B. and G. Roult, Asymptotic approximations for normal modes and surface waves in the vicinity of the antipode: Constraints on global earth models, *J. Geophys. Res.*, **93**, 7885-7896, 1988.

Romanowicz, B. and R. Snieder, A new formalism for the effect of lateral heterogeneity on normal modes and surface waves, II: General anisotropic perturbations, *Geophys. J. R. Astron. Soc.*, **93**, 91-99, 1988.

Smith, M. F. and G. Masters, Aspherical structure constraints from free oscillation frequency and attenuation measurements, *J. Geophys. Res.*, **94**, 1953-1976, 1989.

Snieder, R., On the connection between ray theory and scattering theory for surface waves, in: *Mathematical Geophysics* (N. J. Vlaar, G. Nolet, M. J. R. Wortel and S. A. P. L. Cloetingh, eds.), D. Reidel, 77-84, 1988.

Su, W.-J. and A. M. Dziewonski, Predominance of long wavelength heterogeneity in the mantle, *Nature*, **352**, 121-126, 1991.

Su, W.-J., R. L. Woodward and A. M. Dziewonski, Degreee 12 model of shear velocity heterogeneity in the mantle, *J. Geophys. Res.*, **99**, 6945-6980, 1994.

Takeuchi, H. and M. Saito, Seismic surface waves, in: *Methods Comput. Phys.*, Academic Press, New York, **11**, 217-295, 1972.

Tanimoto, T., A simple derivation of the formula to calculate synthetic long period seismograms in a heterogeneous earth by normal mode summation, *Geophys. J. R. Astron. Soc.*, **77**, 275-278, 1984.

Tanimoto, T., The three dimensional shear wave structure in the mantle by overtone waveform inversion – I. Radial seismogram inversion, *Geophys. J. R. Astron. Soc.*, **89**, 713-740, 1987.

Tanimoto, T., The three dimensional shear wave structure in the mantle by overtone waveform inversion – II. Inversion of X waves, R waves and G waves, *Geophys. J. R. Astron. Soc.*, **93**, 321-333, 1988.

Tanimoto, T., Long wavelength S-velocity structure throughout the mantle, *Geophys. J. Int.*, **100**, 327-336, 1990.

Um, J., and F. A. Dahlen, Normal mode multiplet coupling on an anelastic Earth, *Geophys. J. Int.*, in press, 1992.

Valette, B., About the influence of pre-stress upon adiabatic perturbations of the Earth, *Geophys. J. R. astr. Soc.*, **85**, 179-208, 1986.

Watson, G. N., The diffraction of electric waves by the Earth, *Proc. R. Soc. Lond.*, **A95**, 83, 1918.

Widmer, R., G. Masters and F. Gilbert, Observably split multiplets – data analysis and interpretation in terms of large scale structure, *Geophys. J. Int.*, **111**, 559-576, 1992.

Wong, Y. K., *Upper mantle heterogeneity from phase and amplitude data of mantle waves*, Ph.D. Thesis, Harvard Univ., Cambridge, Massachusetts, 1989.

Woodhouse, J. H., Surface waves in a laterally varying layered structure, *Geophys. J. R. Astron. Soc.*, **37**, 461-490, 1974.

Woodhouse, J. H., On Rayleigh's principle, *Geophys. J. R. Astron. Soc.*, **46**, 11-22, 1976.

Woodhouse, J. H., Asymptotic results for elastodynamic propagator matrices in plane stratified and spherically stratified Earth-models, *Geophys. J. R. Astron. Soc.*, **54**, 263-280, 1978.

Woodhouse, J. H., The coupling and attenuation of nearly resonant multiplets in the earth's free oscillation spectrum, *Geophys. J. R. Astron. Soc.*, **61**, 261-283, 1980.

Woodhouse, J. H., The joint inversion of seismic waveforms for lateral variations in Earth structure and earthquake source parameters, Proc. "Enrico Fermi" Int. Sch. Phys. *LXXXV* (H. Kanamori and E. Boschi, eds.), 366-397, 1983.

Woodhouse, J. H., The calculation of the eigenfrequencies and eigenfunctions of the free oscillations of the Earth and the Sun, in: *Seismological Algorithms* (D. J. Doornbos, ed.), 321-370, 1988.

Woodhouse, J. H. and F. A. Dahlen, The effect of a general aspherical perturbation on the free oscillations of the Earth, *Geophys. J. R. astr. Soc.*, **53**, 335-354, 1978.

Woodhouse, J. H. and A. M. Dziewonski, Mapping the upper mantle: Three dimensional modelling of Earth structure by inversion of seismic waveforms, *J. Geophys. Res.*, **89**, 5953-5986, 1984.

Woodhouse, J. H. and A. M. Dziewonski, Three dimensional mantle models based on mantle wave and long period body wave data, *EOS, Trans. Am. Geophys. Un.*, **67**, 307, 1986.

Woodhouse, J. H. and A. M. Dziewonski, Seismic modelling of the Earth's large-scale three dimensional structure, *Philos. Trans. R. Soc. Lond. A*, **328**, 291-308, 1989.

Woodhouse, J. H. and T. P. Girnius, Surface waves and free oscillations in a regionalized Earth model, *Geophys. J. R. Astron. Soc.*, **68**, 653-673, 1982.

Woodhouse, J. H. and Y. K. Wong, Amplitude, phase and path anomalies of mantle waves, *Geophys. J. R. Astron. Soc.*, **87**, 753-773, 1986.

Woodhouse, J. H., D. Giardini and X. D. Li, Evidence for inner core anisotropy from free oscillations, *Geophys. Res. Lett.*, **13**, 1549-1552, 1986.

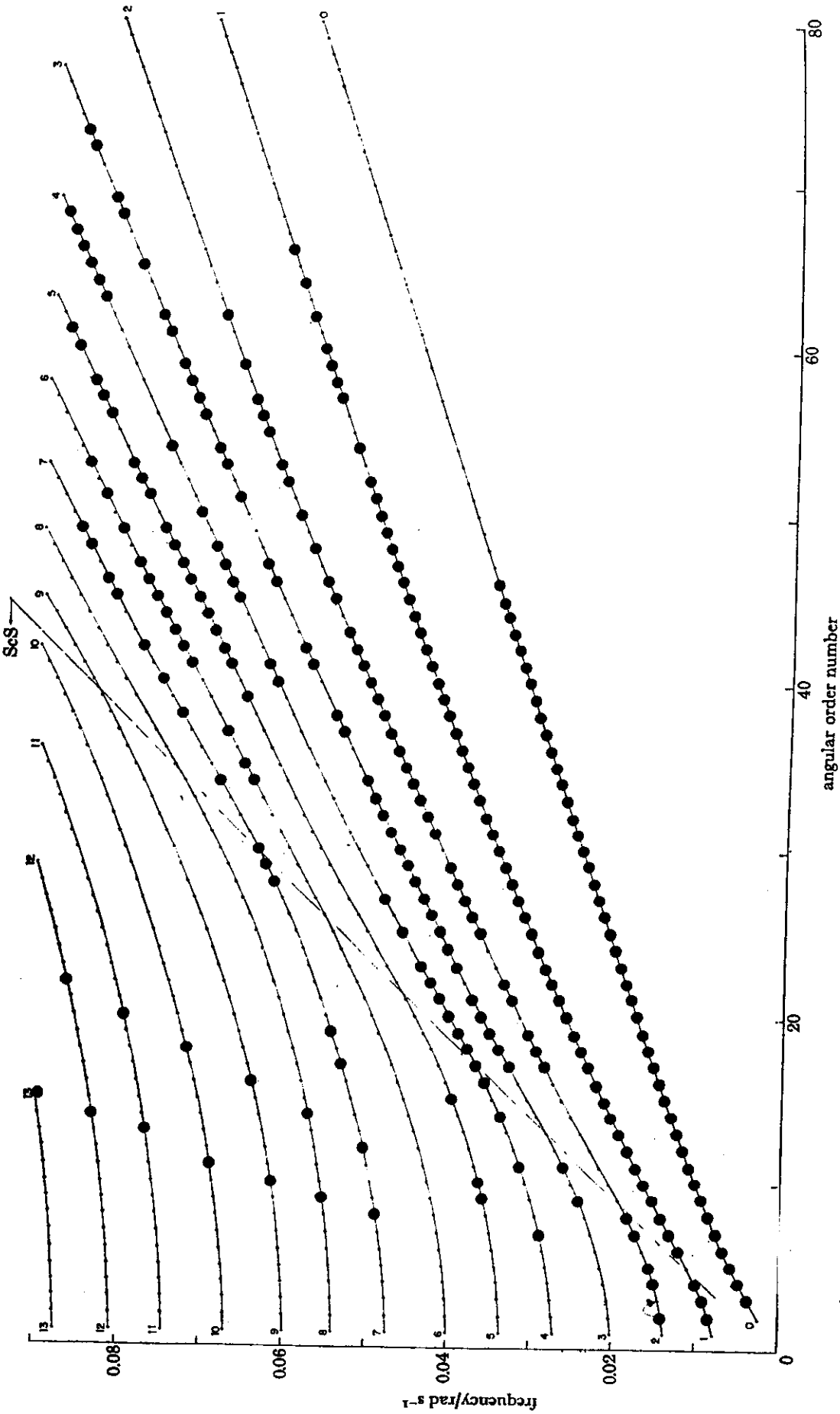

Toroidal normal modes in the (ω, l) plane. The large dots indicate observed modes used in the inversions. Most of the toroidal overtones identified by Brune & Gilbert (1964) fall outside the range of the figure. The dashed line designated 'ScS' divides the modes into two groups according to the normal mode–body wave analogy: modes to the left of this line correspond to $(ScS)_H$ reflexions, those to the right correspond to mantle S_H waves.

Fig 1a

Fig 1b

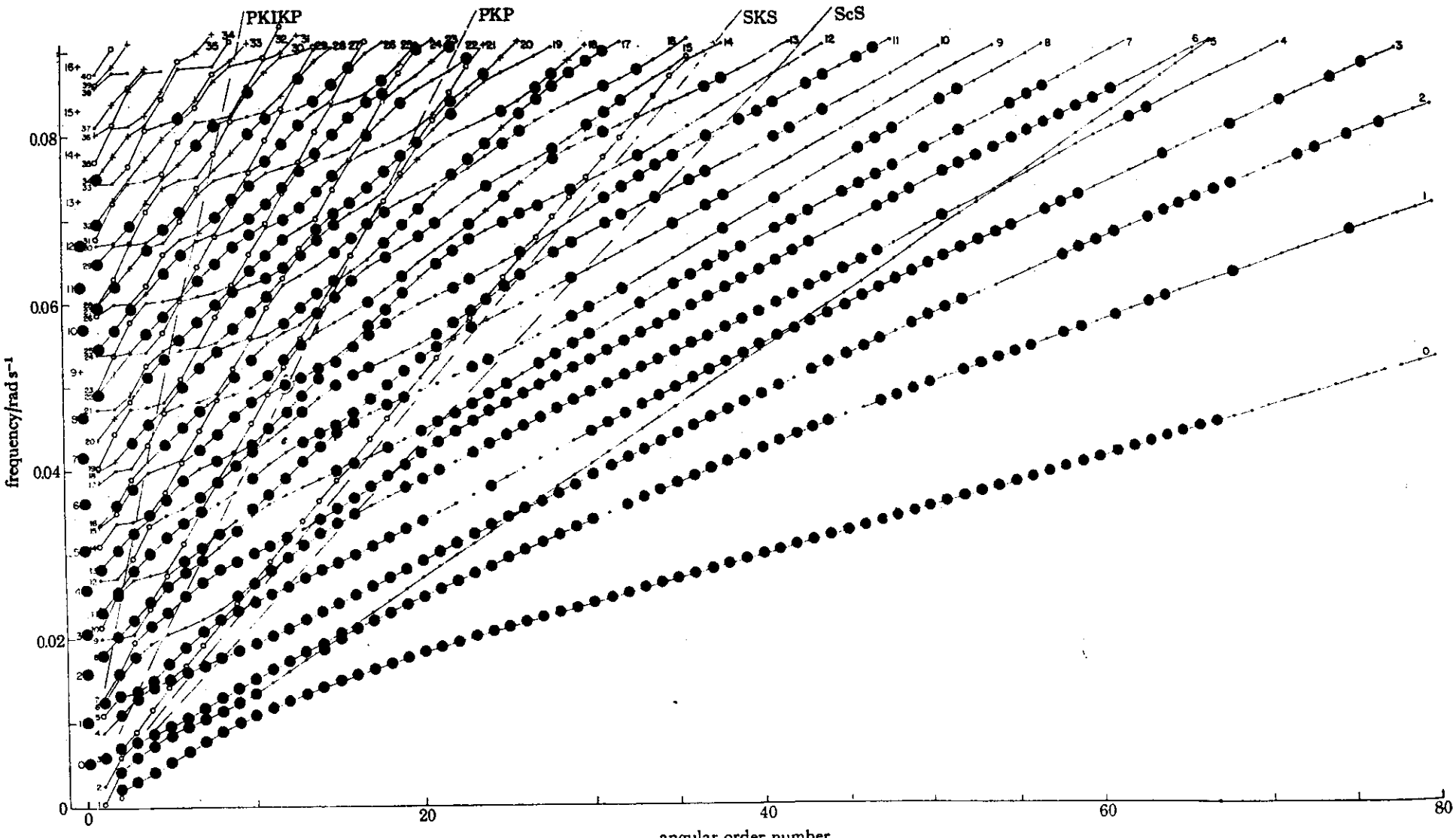

Spheroidal normal modes in the (ω, l) plane. The large dots indicate observed modes used in the inversions. For further details we refer the reader to §3 of Alaska II. •, $CE < 0.5$; +, $CE \geq 0.5$; ○ core modes.

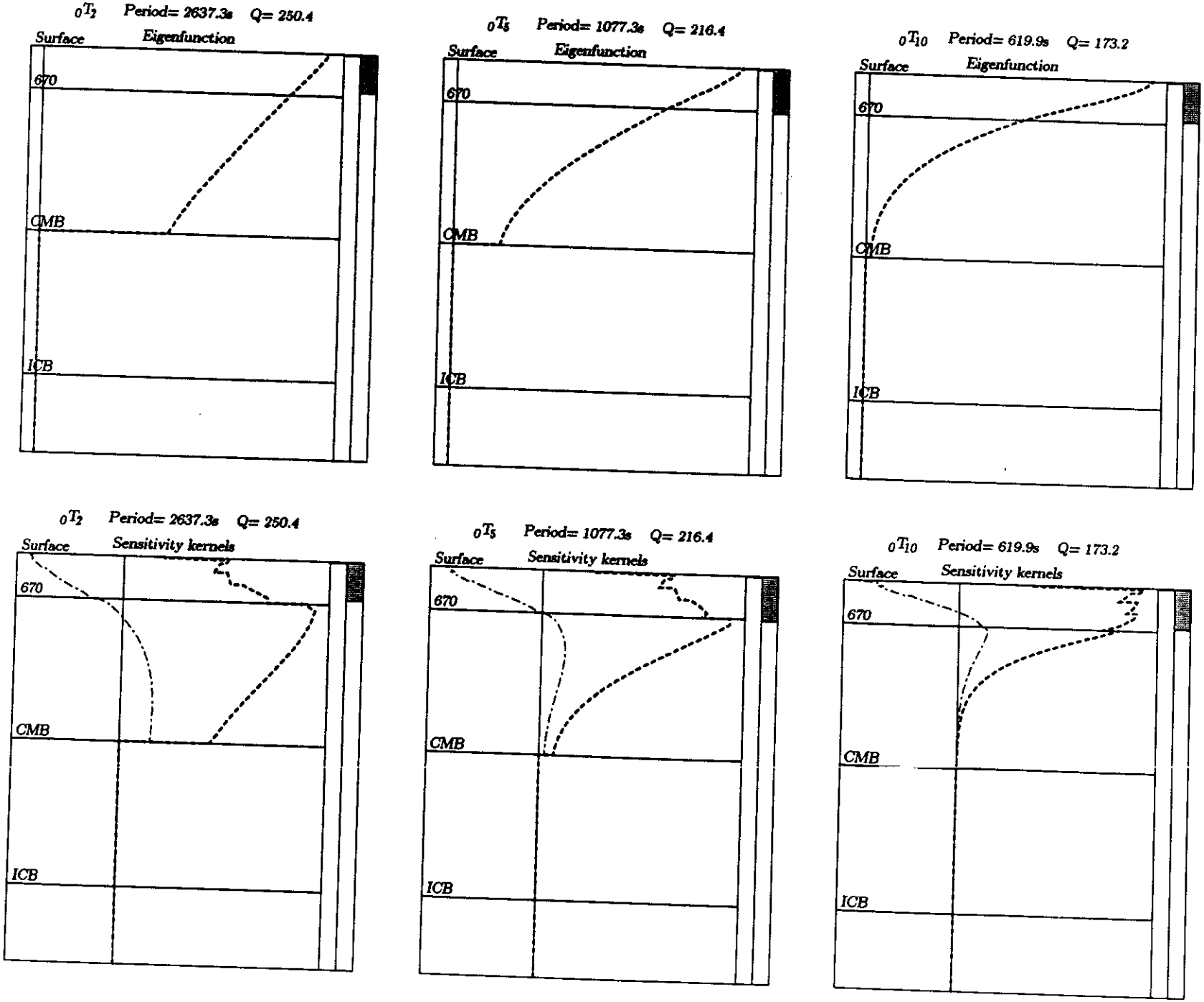
$_0T_2$ Period= 2637.3s Q= 250.4
Surface Eigenfunction
670
CMB
ICB
$_0T_5$ Period= 1077.3s Q= 216.4
Surface Eigenfunction
670
CMB
ICB
$_0T_{10}$ Period= 619.9s Q= 173.2
Surface Eigenfunction
670
CMB
ICB
$_0T_2$ Period= 2637.3s Q= 250.4
Surface Sensitivity kernels
670
CMB
ICB
$_0T_5$ Period= 1077.3s Q= 216.4
Surface Sensitivity kernels
670
CMB
ICB
$_0T_{10}$ Period= 619.9s Q= 173.2
Surface Sensitivity kernels
670
CMB
ICB

Fig 2a

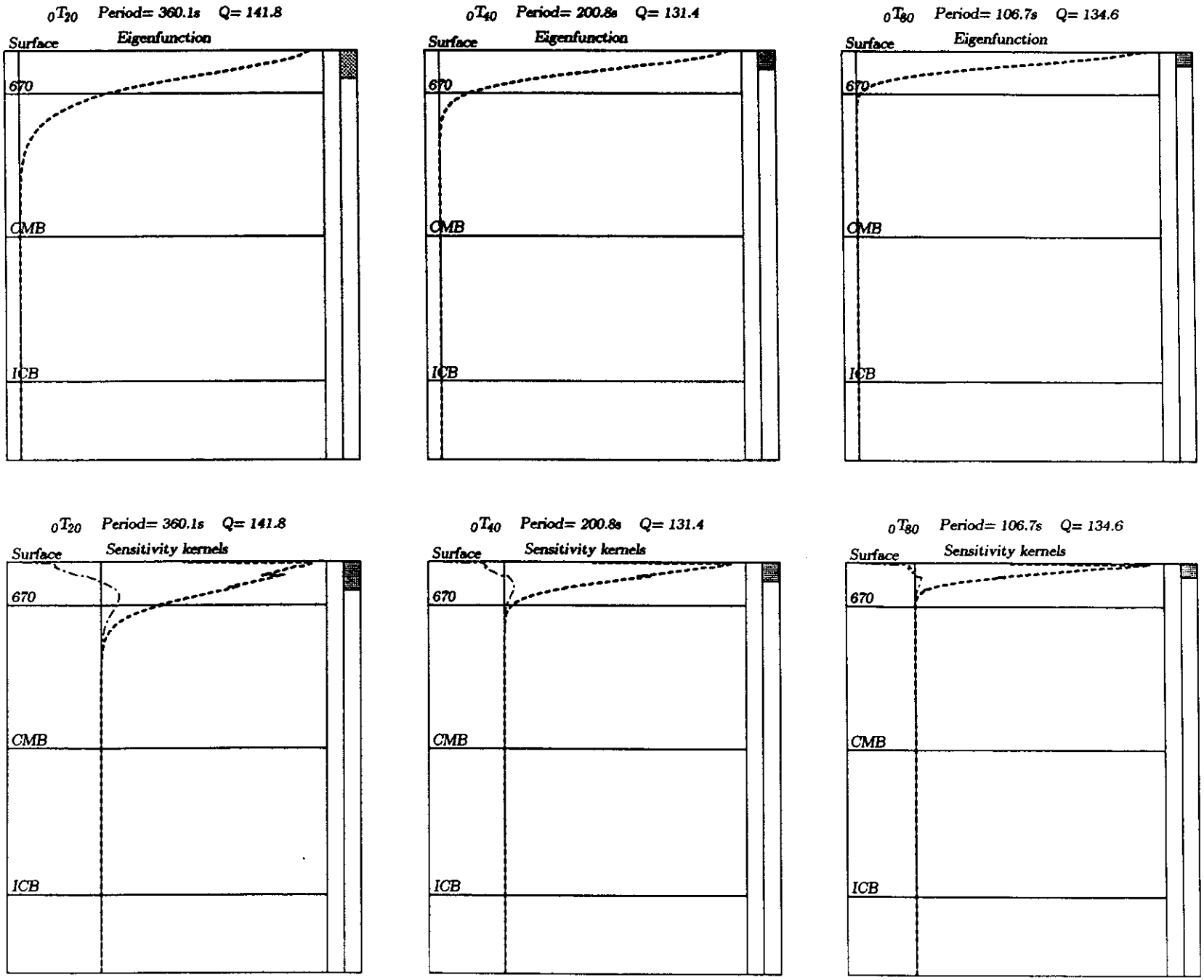
$_0T_{20}$ Period= 360.1s Q= 141.8
Surface
Eigenfunction
670
CMB
ICB
$_0T_{40}$ Period= 200.8s Q= 131.4
Surface
Eigenfunction
670
CMB
ICB
$_0T_{80}$ Period= 106.7s Q= 134.6
Surface
Eigenfunction
670
CMB
ICB
$_0T_{20}$ Period= 360.1s Q= 141.8
Surface
Sensitivity kernels
670
CMB
ICB
$_0T_{40}$ Period= 200.8s Q= 131.4
Surface
Sensitivity kernels
670
CMB
ICB
$_0T_{80}$ Period= 106.7s Q= 134.6
Surface
Sensitivity kernels
670
CMB
ICB

Fig 2a. cont.

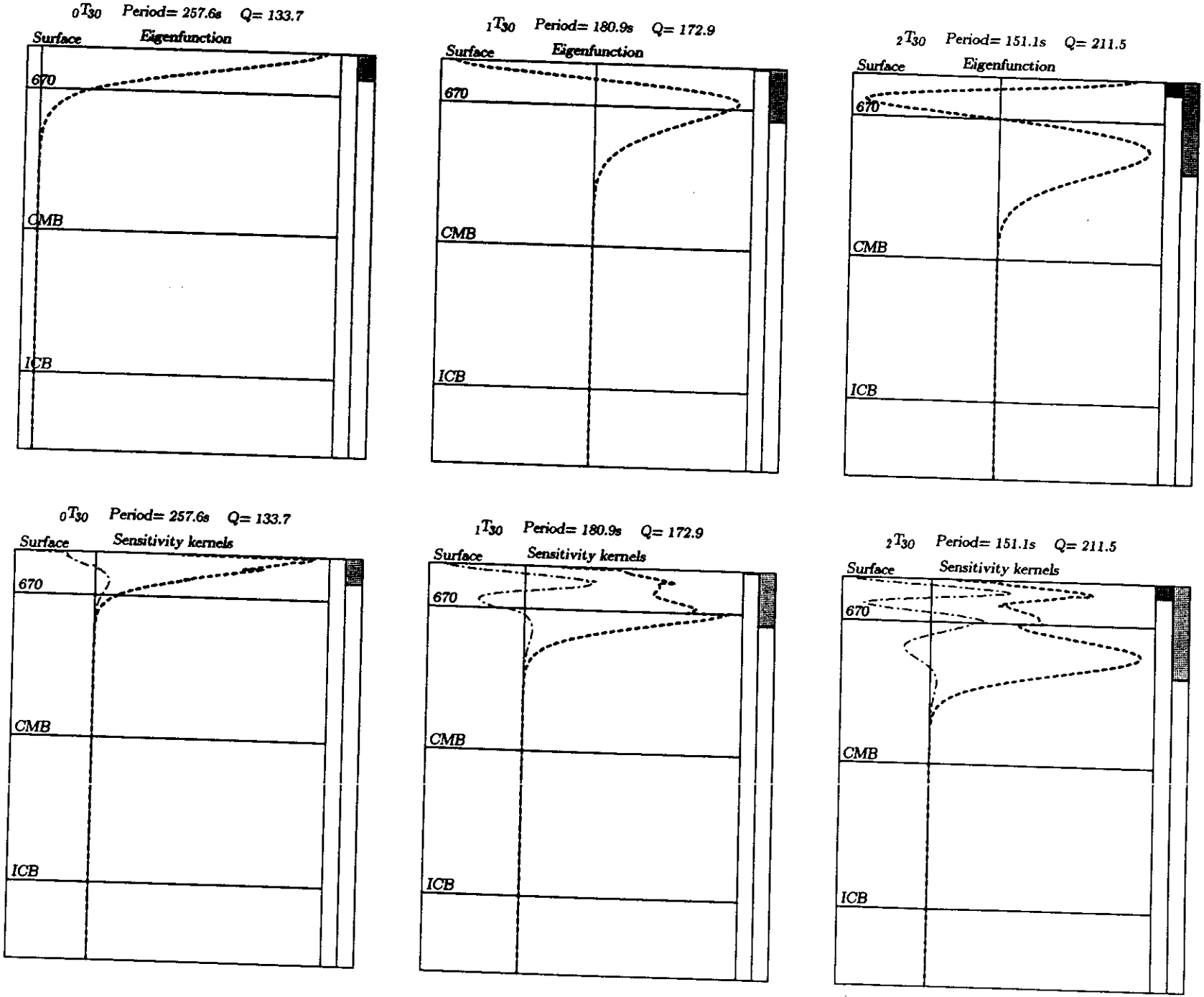
$_0T_{30}$ Period= 257.6s Q= 133.7
Surface
Eigenfunction
670
CMB
ICB
$_1T_{30}$ Period= 180.9s Q= 172.9
Surface
Eigenfunction
670
CMB
ICB
$_2T_{30}$ Period= 151.1s Q= 211.5
Surface
Eigenfunction
670
CMB
ICB
$_0T_{30}$ Period= 257.6s Q= 133.7
Surface
Sensitivity kernels
670
CMB
ICB
$_1T_{30}$ Period= 180.9s Q= 172.9
Surface
Sensitivity kernels
670
CMB
ICB
$_2T_{30}$ Period= 151.1s Q= 211.5
Surface
Sensitivity kernels
670
CMB
ICB

Fig 2b

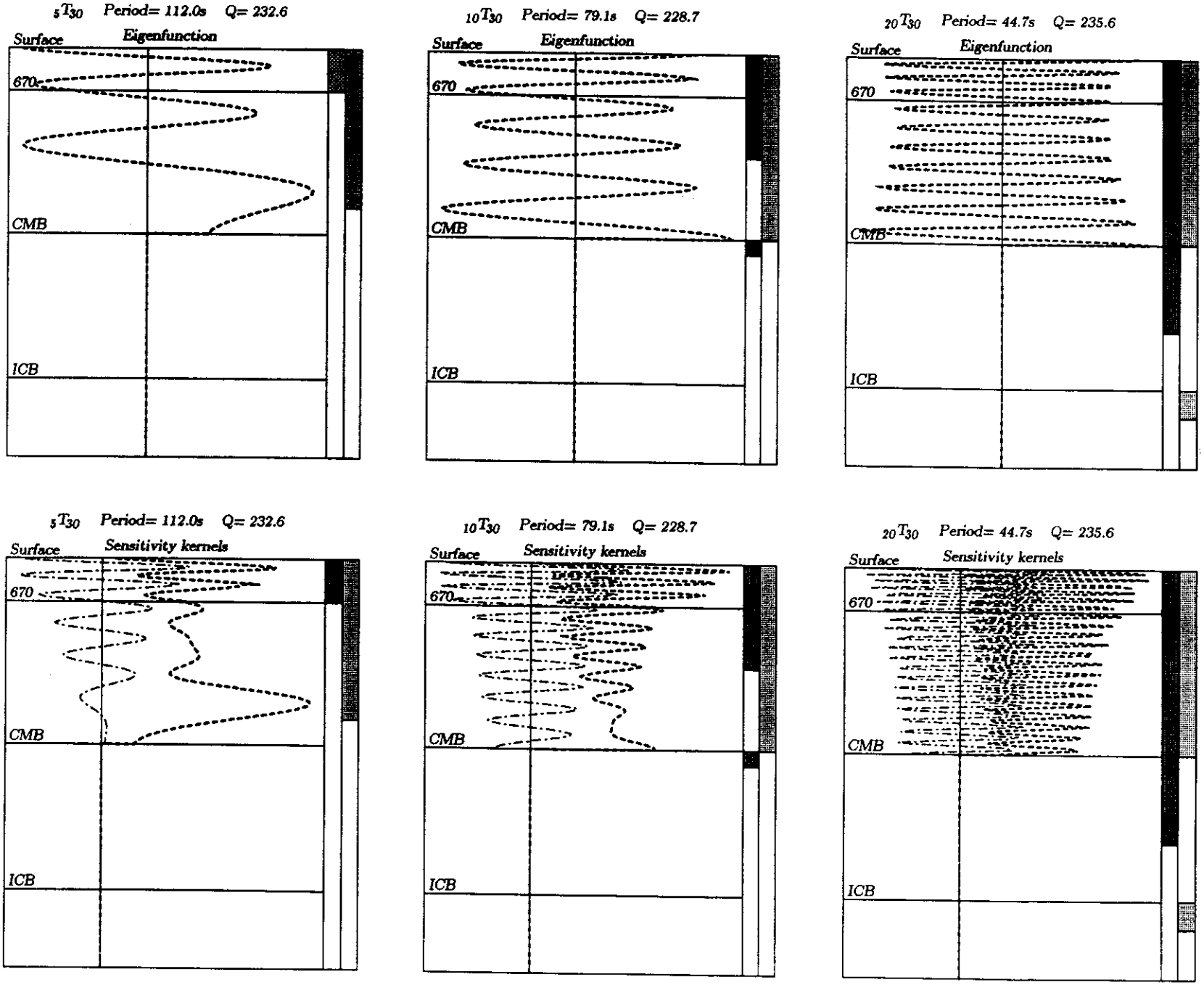
$_5T_{30}$ Period= 112.0s Q= 232.6
Surface
Eigenfunction
670
CMB
ICB
$_{10}T_{30}$ Period= 79.1s Q= 228.7
Surface
Eigenfunction
670
CMB
ICB
$_{20}T_{30}$ Period= 44.7s Q= 235.6
Surface
Eigenfunction
670
CMB
ICB
$_5T_{30}$ Period= 112.0s Q= 232.6
Surface
Sensitivity kernels
670
CMB
ICB
$_{10}T_{30}$ Period= 79.1s Q= 228.7
Surface
Sensitivity kernels
670
CMB
ICB
$_{20}T_{30}$ Period= 44.7s Q= 235.6
Surface
Sensitivity kernels
670
CMB
ICB

Fig 2b cont.

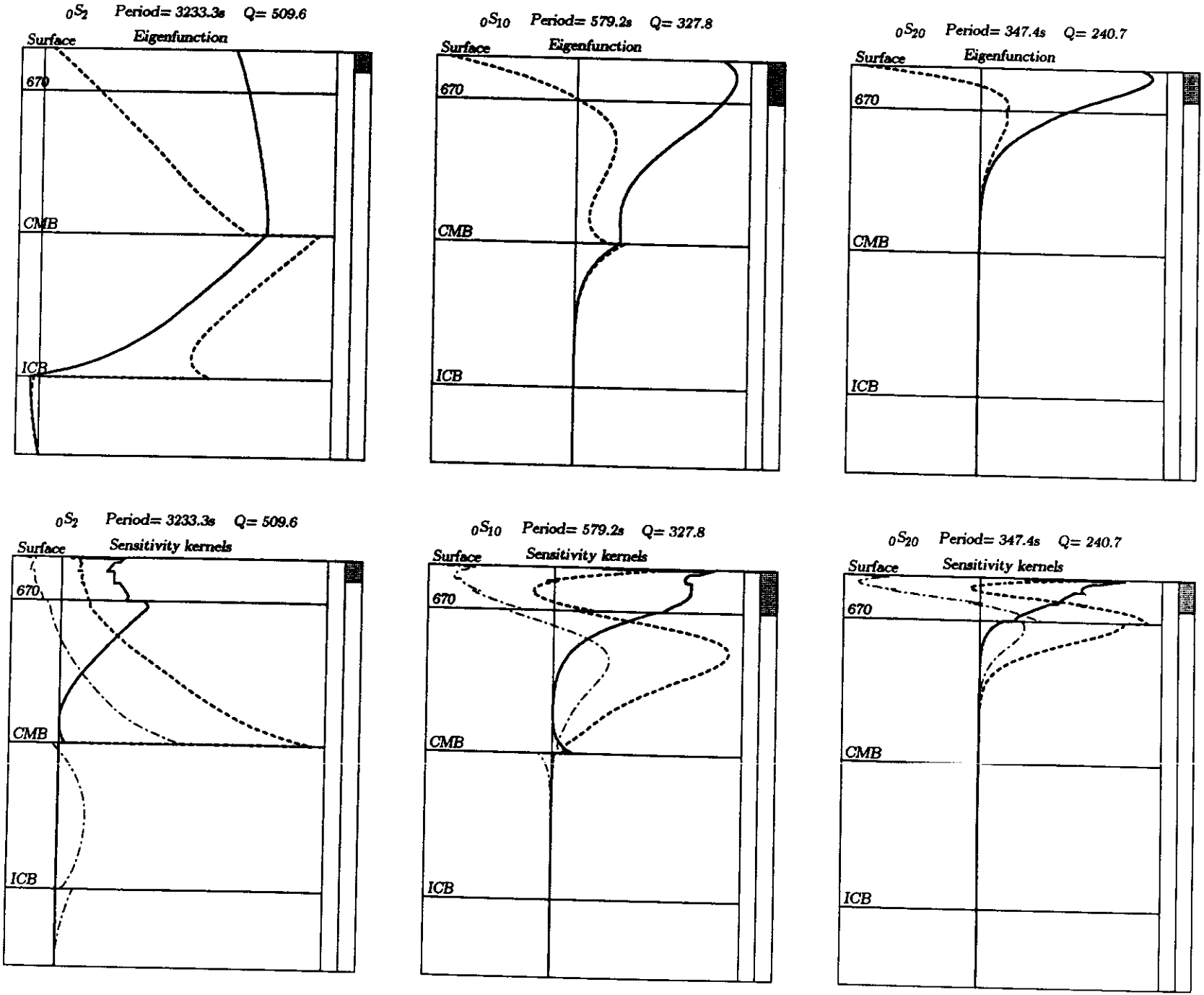
$_0S_2$ Period= 3233.3s Q= 509.6
Surface
Eigenfunction
670
CMB
ICB
$_0S_{10}$ Period= 579.2s Q= 327.8
Surface
Eigenfunction
670
CMB
ICB
$_0S_{20}$ Period= 347.4s Q= 240.7
Surface
Eigenfunction
670
CMB
ICB
$_0S_2$ Period= 3233.3s Q= 509.6
Surface
Sensitivity kernels
670
CMB
ICB
$_0S_{10}$ Period= 579.2s Q= 327.8
Surface
Sensitivity kernels
670
CMB
ICB
$_0S_{20}$ Period= 347.4s Q= 240.7
Surface
Sensitivity kernels
670
CMB
ICB

Fig 2c

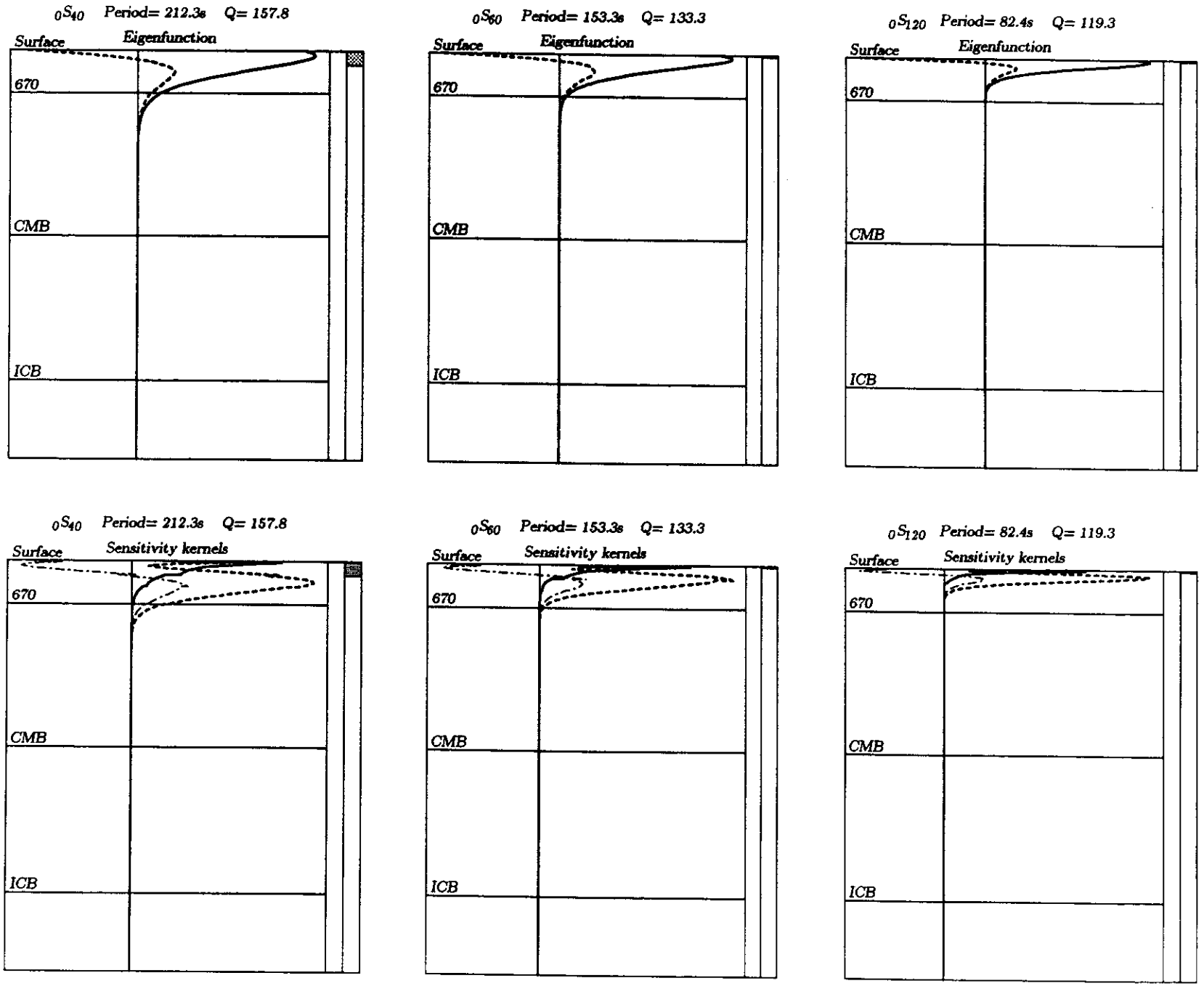
$_0S_{40}$ Period= 212.3s Q= 157.8
Surface
Eigenfunction
670
CMB
ICB
$_0S_{60}$ Period= 153.3s Q= 133.3
Surface
Eigenfunction
670
CMB
ICB
$_0S_{120}$ Period= 82.4s Q= 119.3
Surface
Eigenfunction
670
CMB
ICB
$_0S_{40}$ Period= 212.3s Q= 157.8
Surface
Sensitivity kernels
670
CMB
ICB
$_0S_{60}$ Period= 153.3s Q= 133.3
Surface
Sensitivity kernels
670
CMB
ICB
$_0S_{120}$ Period= 82.4s Q= 119.3
Surface
Sensitivity kernels
670
CMB
ICB

Fig 2c cont.

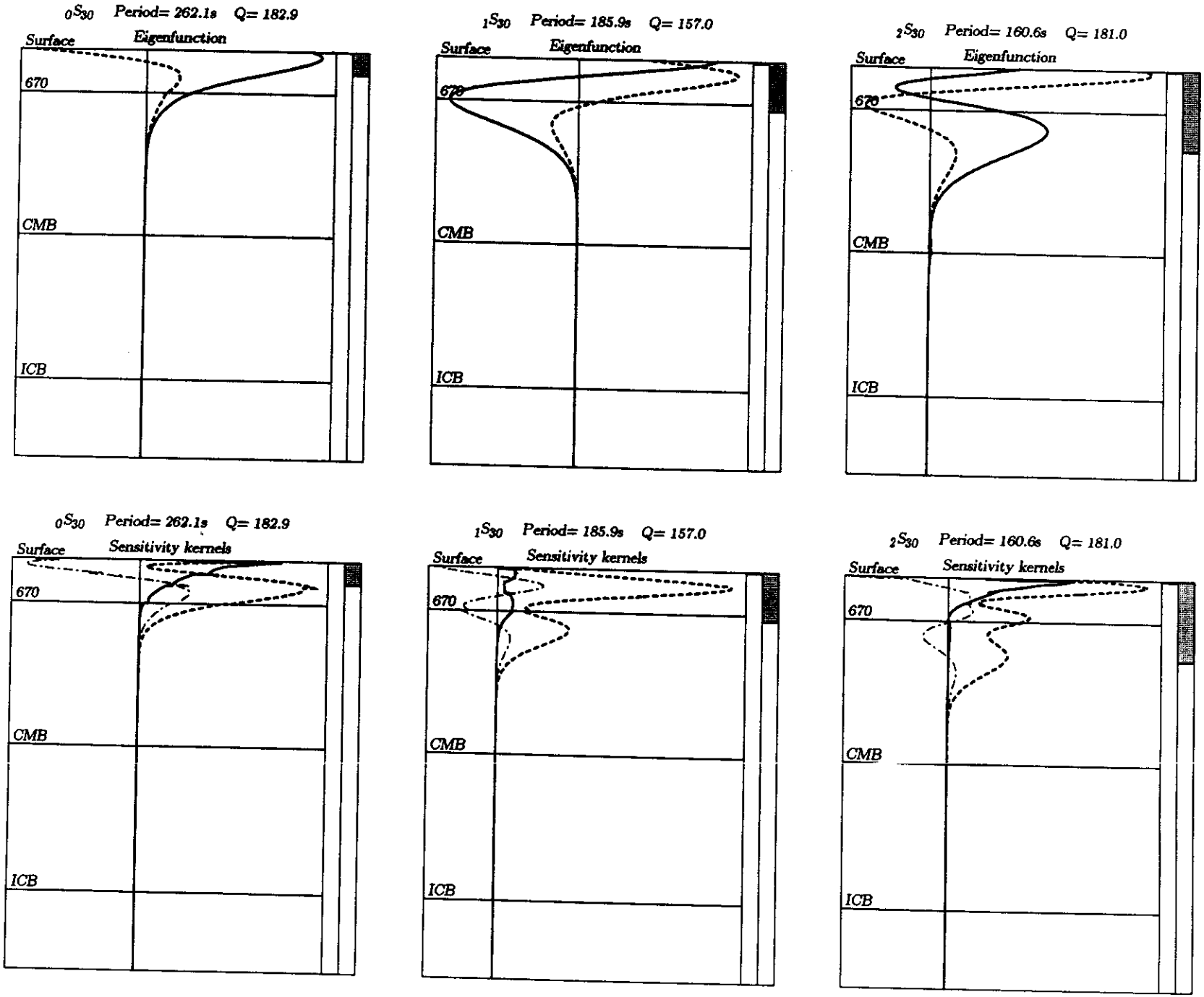
$_0S_{30}$ Period= 262.1s Q= 182.9
Surface
Eigenfunction
670
CMB
ICB
$_1S_{30}$ Period= 185.9s Q= 157.0
Surface
Eigenfunction
670
CMB
ICB
$_2S_{30}$ Period= 160.6s Q= 181.0
Surface
Eigenfunction
670
CMB
ICB
$_0S_{30}$ Period= 262.1s Q= 182.9
Surface
Sensitivity kernels
670
CMB
ICB
$_1S_{30}$ Period= 185.9s Q= 157.0
Surface
Sensitivity kernels
670
CMB
ICB
$_2S_{30}$ Period= 160.6s Q= 181.0
Surface
Sensitivity kernels
670
CMB
ICB

Fig 2d

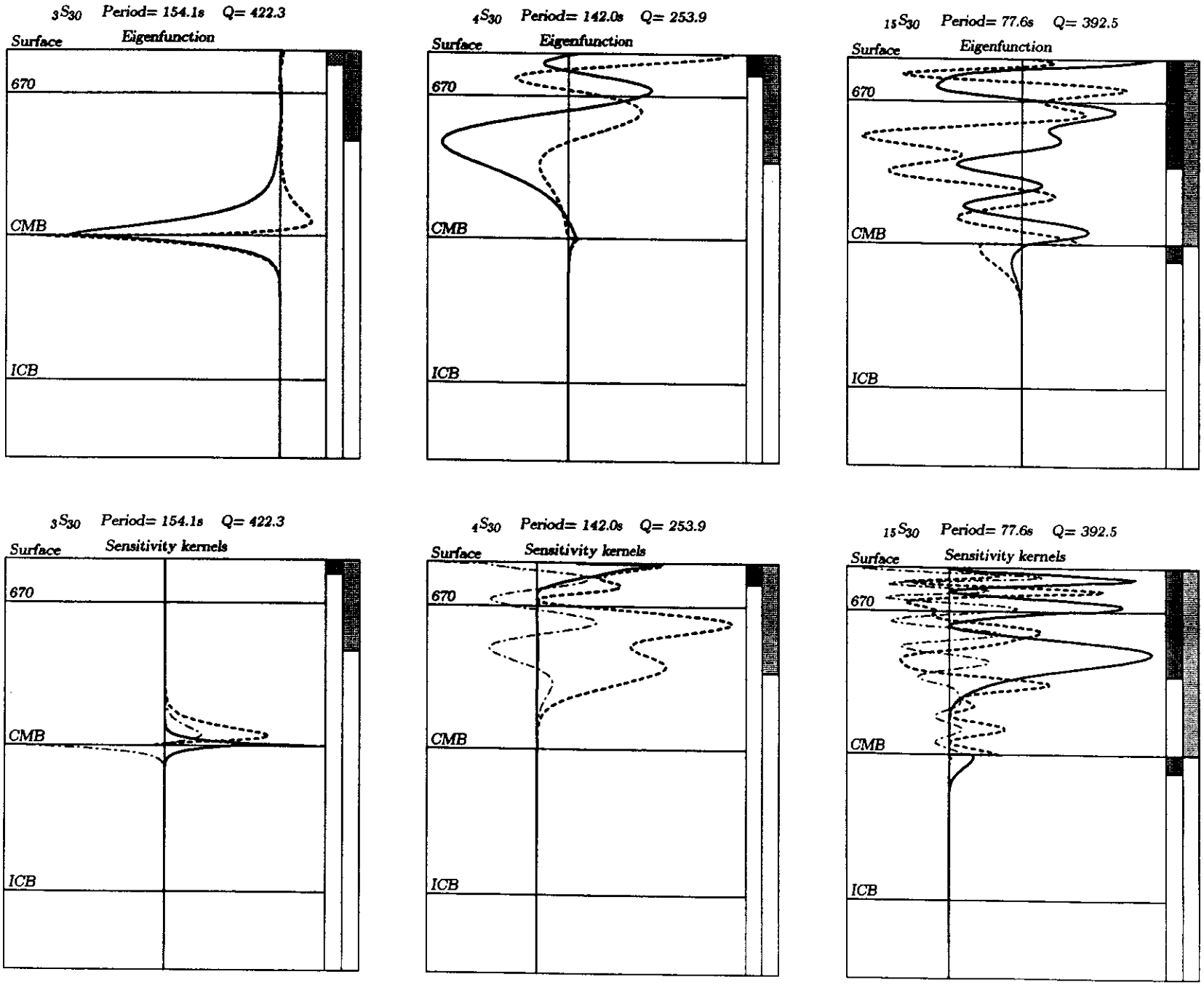
$_3S_{30}$ Period= 154.1s Q= 422.3
Surface
Eigenfunction
670
CMB
ICB
$_4S_{30}$ Period= 142.0s Q= 253.9
Surface
Eigenfunction
670
CMB
ICB
$_{15}S_{30}$ Period= 77.6s Q= 392.5
Surface
Eigenfunction
670
CMB
ICB
$_3S_{30}$ Period= 154.1s Q= 422.3
Surface
Sensitivity kernels
670
CMB
ICB
$_4S_{30}$ Period= 142.0s Q= 253.9
Surface
Sensitivity kernels
670
CMB
ICB
$_{15}S_{30}$ Period= 77.6s Q= 392.5
Surface
Sensitivity kernels
670
CMB
ICB

Fig 2d cont.

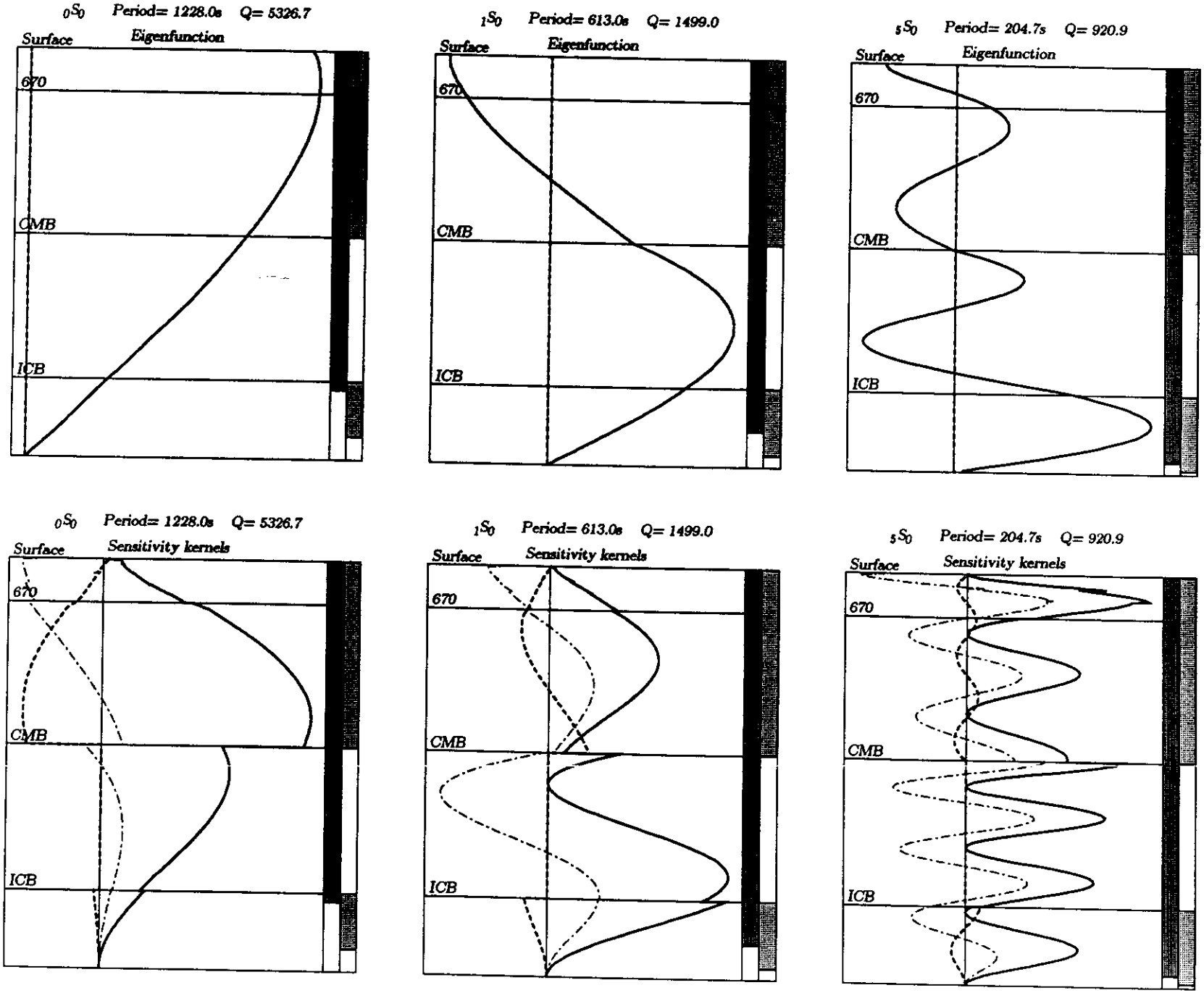
$_0S_0$ Period= 1228.0s Q= 5326.7
Surface
Eigenfunction
670
CMB
ICB
$_1S_0$ Period= 613.0s Q= 1499.0
Surface
Eigenfunction
670
CMB
ICB
$_5S_0$ Period= 204.7s Q= 920.9
Surface
Eigenfunction
670
CMB
ICB
$_0S_0$ Period= 1228.0s Q= 5326.7
Surface
Sensitivity kernels
670
CMB
ICB
$_1S_0$ Period= 613.0s Q= 1499.0
Surface
Sensitivity kernels
670
CMB
ICB
$_5S_0$ Period= 204.7s Q= 920.9
Surface
Sensitivity kernels
670
CMB
ICB

Fig 2e

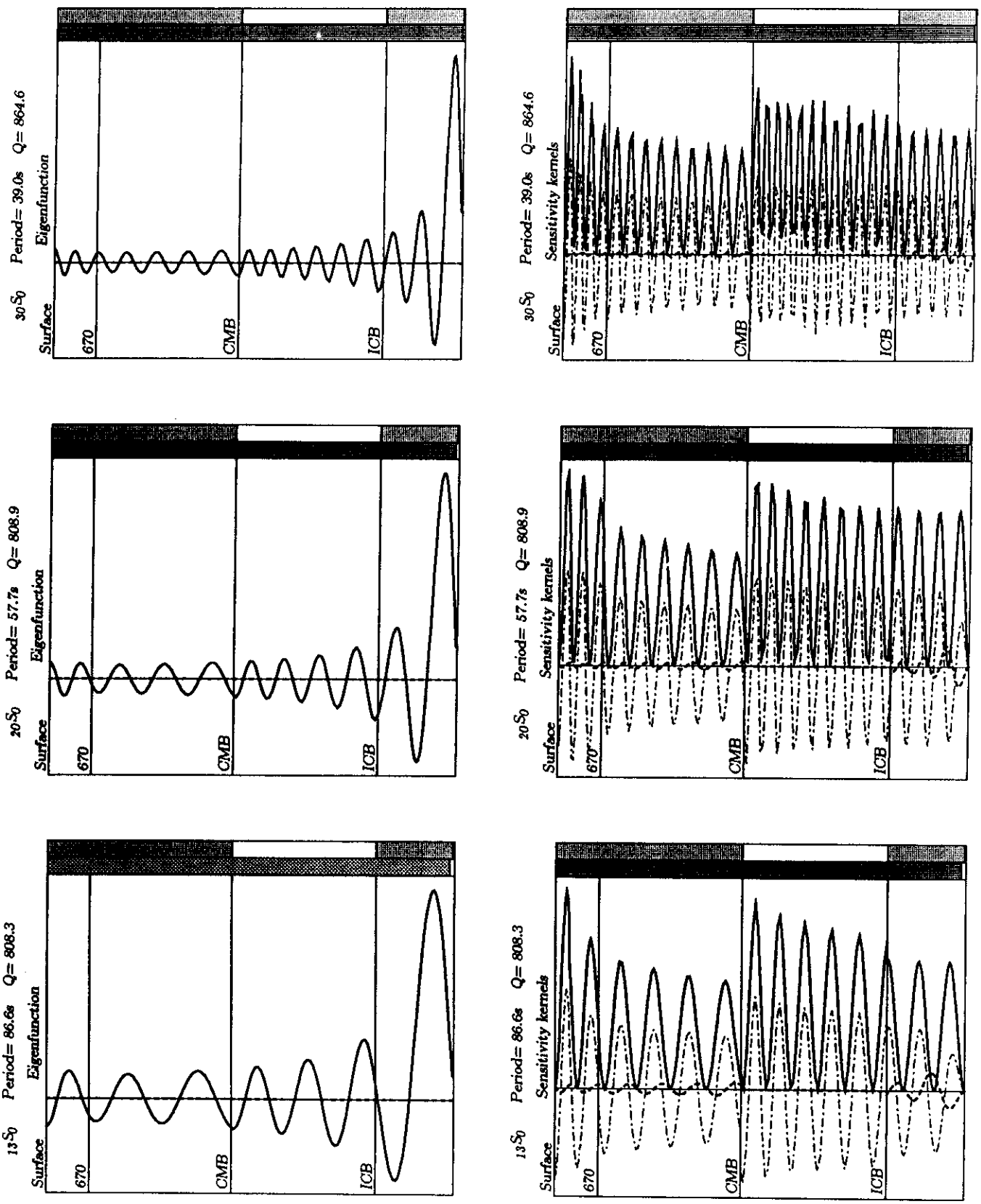
30S0 Period= 39.0s Q= 864.6 Eigenfunction
Surface
670
CMB
ICB
30S0 Period= 39.0s Q= 864.6 Sensitivity kernels
Surface
670
CMB
ICB
20S0 Period= 57.7s Q= 808.9 Eigenfunction
Surface
670
CMB
ICB
20S0 Period= 57.7s Q= 808.9 Sensitivity kernels
Surface
670
CMB
ICB
13S0 Period= 86.6s Q= 808.3 Eigenfunction
Surface
670
CMB
ICB
13S0 Period= 86.6s Q= 808.3 Sensitivity kernels
Surface
670
CMB
ICB

Fig 2e cont.

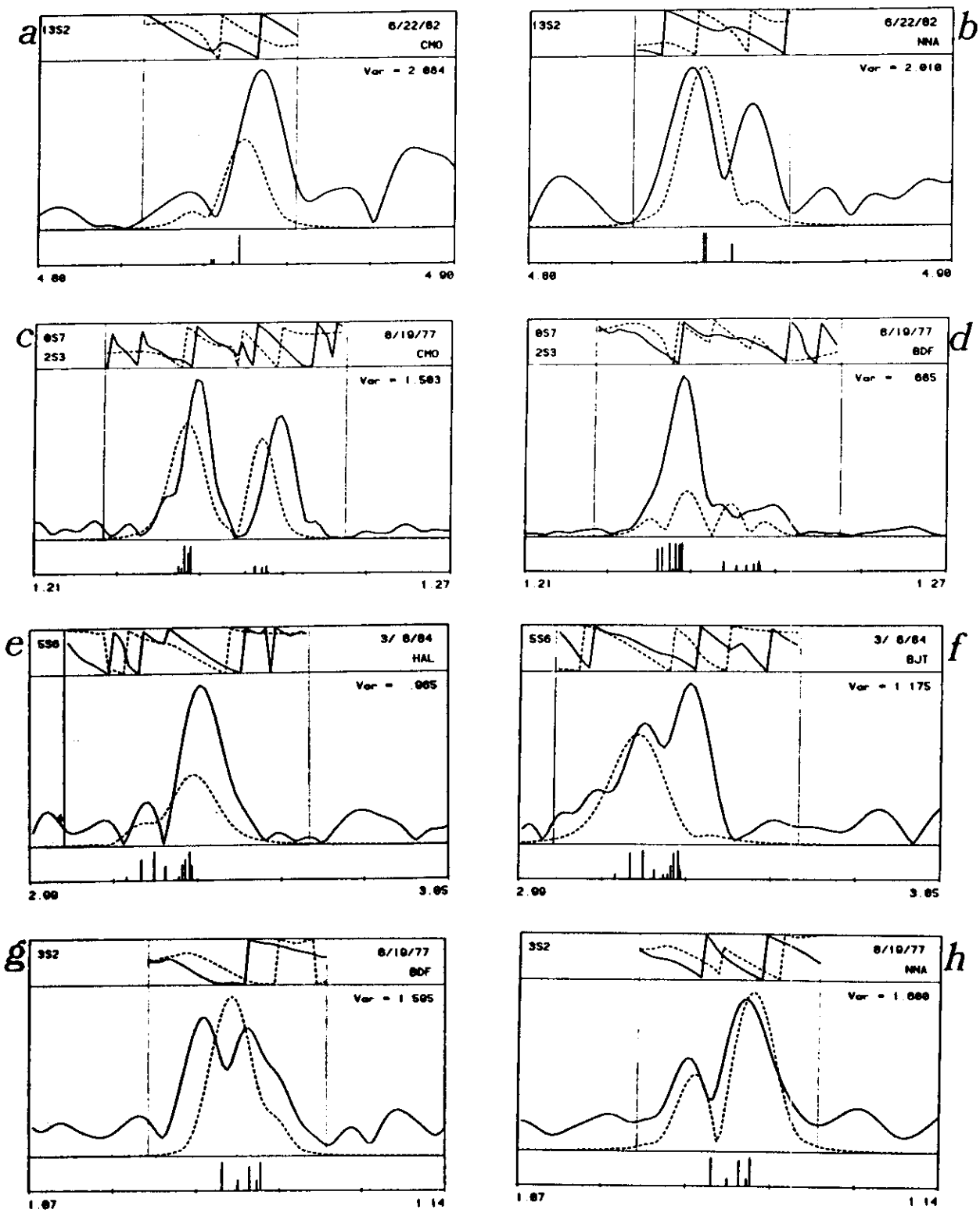

Examples of data (solid lines) and synthetic spectra (dashed lines) in spectral windows containing one or two modes. For each window are indicated the name(s) of the multiplet(s), the range of the horizontal frequency axis (in millihertz), the earthquake date, and the recording station. The complex spectra are represented in terms of phase in the interval $(-\pi, \pi)$ (top panel of each figure), and amplitude on an arbitrary scale (middle panel). Vertical bars in the bottom panels indicate the frequencies and relative amplitudes of the singlets contributing to the theoretical spectra, computed for the reference model PREM, incorporating the effects of rotation and ellipticity. Vertical dotted lines delineate the portion of the signal used in the inversion. The variance ratio is a measure of the misfit between the observed and synthetic traces, computed in terms of the complex spectra. The durations and starting times (relative to event origin time) of each record are, respectively, (*a*) 48, 6, (*b*) 48, 6, (*c*) 140, 5.6, (*d*) 140, 14.8, (*e*) 80, 1.4, (*f*) 80, 1.6, (*g*) 80, 15, and (*h*) 60, 7, all in hours.

Fig 3.

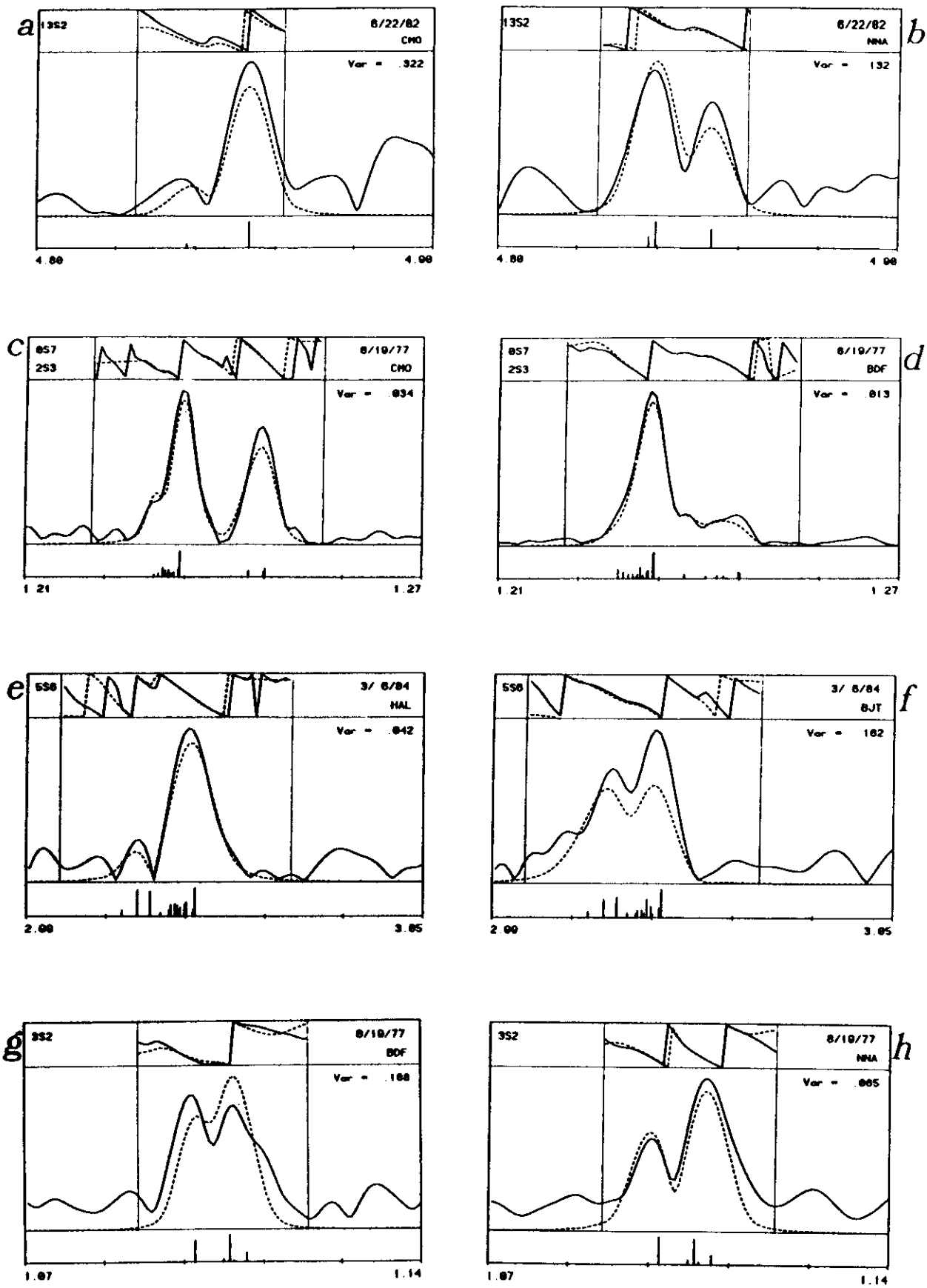

Data (solid lines) and synthetic spectra (dashed lines), as in Figure 1, but with the synthetic spectra obtained using the splitting functions of Table 4. See caption to Figure 1.

Fig 4.

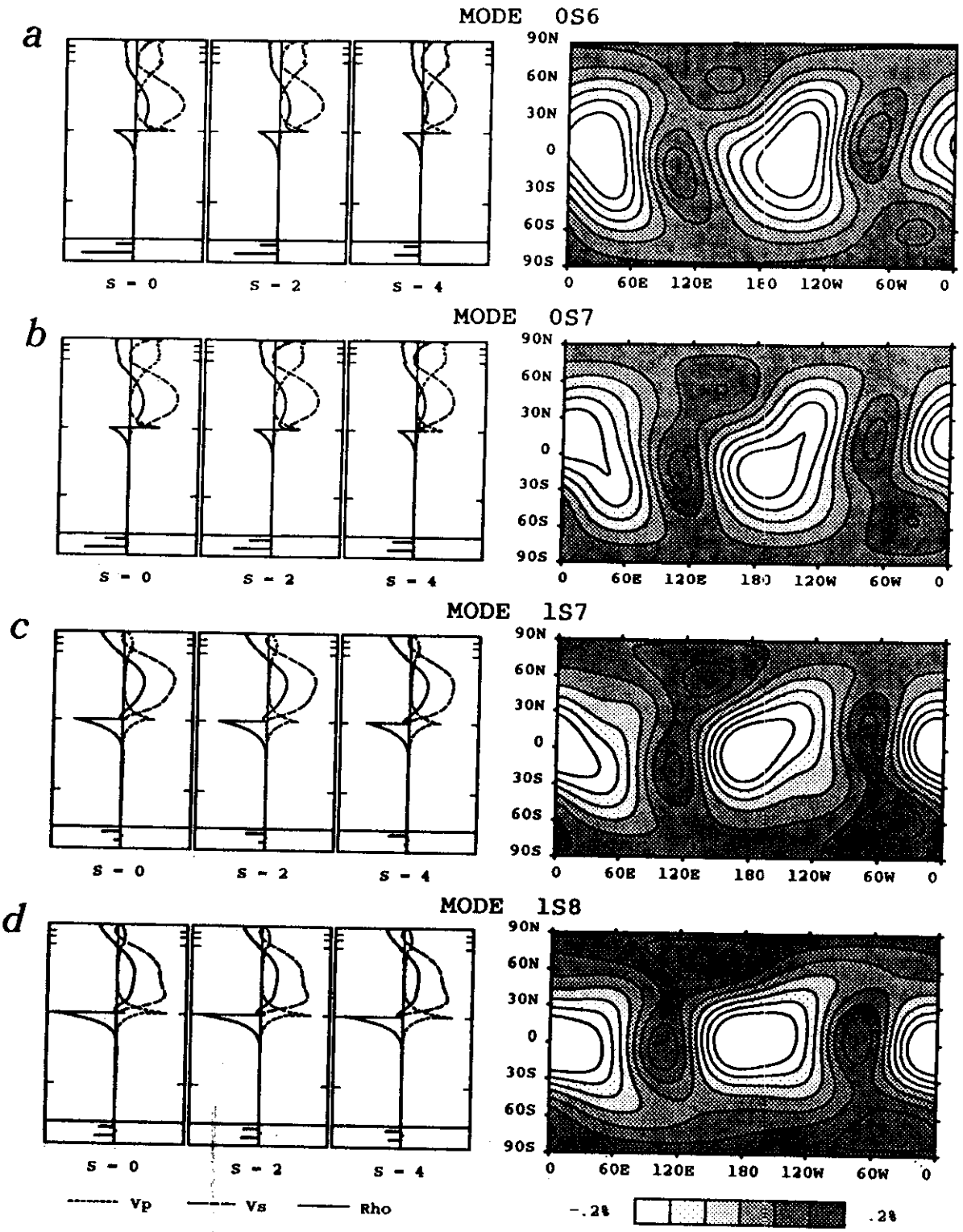

Differential kernels and splitting functions for modes ${}_0S_6$, ${}_0S_7$, ${}_1S_7$, and ${}_1S_8$, dominated by sensitivity to v_S structure in the lower mantle and having large kernels in the outermost core and in the proximity of the core-mantle boundary. See caption to Figure 7 for details.

Fig 5.

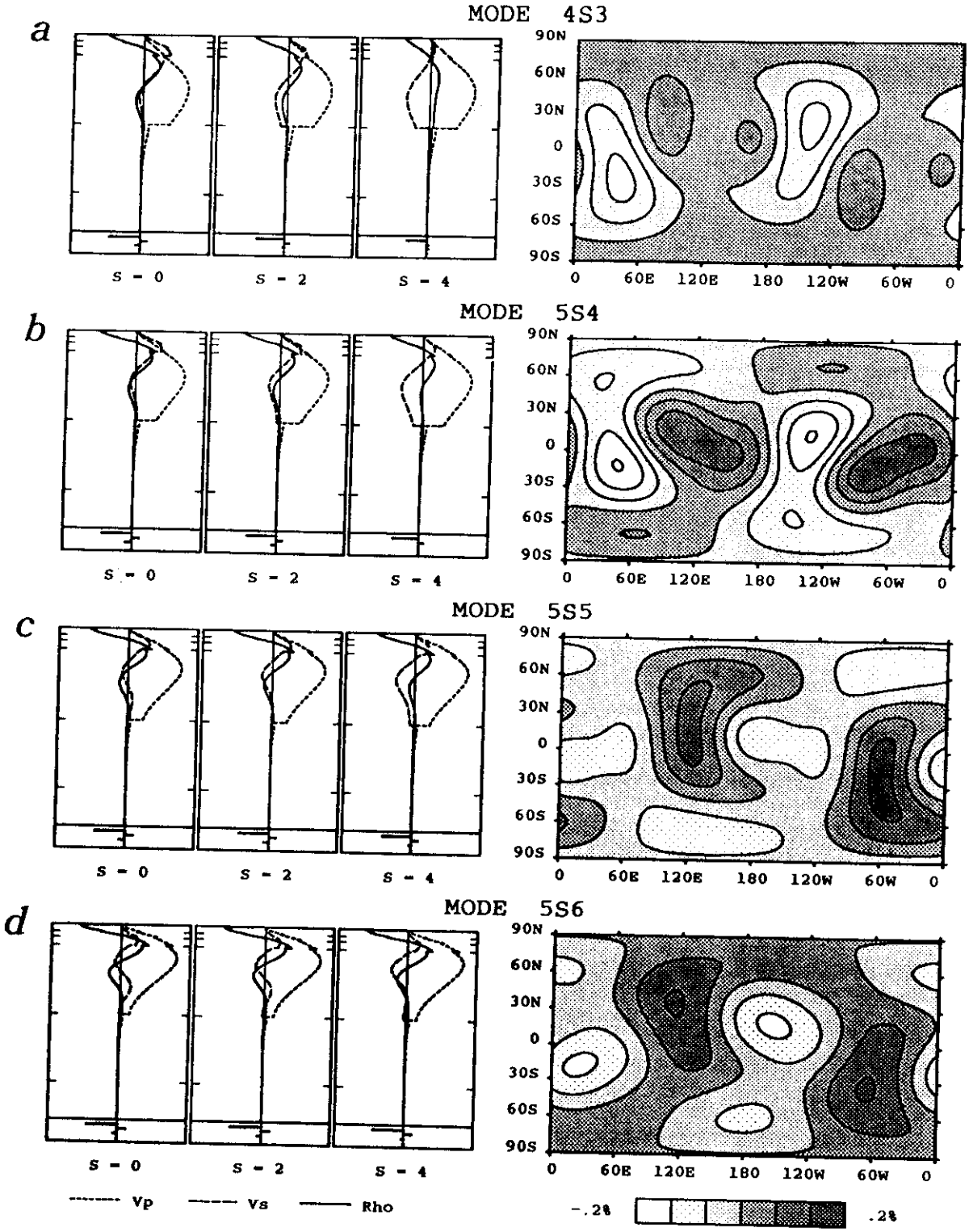

Differential kernels and splitting functions for modes ${}_4S_3$, ${}_5S_4$, ${}_5S_5$, and ${}_5S_6$. The differential kernels represent the sensitivity, as a function of depth, of the splitting function elements to a 1% perturbation in v_P, v_S, and ρ. For a given mode the kernels are independent of angular order t, and only weakly dependent on degree s for high l modes. Here we show separate kernels for degree $s = 0, 2, 4$ and for v_P, v_S, and ρ, centered on the 0 line. At the bottom of each panel we also show the sensitivity to topographic perturbations of the four major surfaces of discontinuity; from top to bottom, these are the free surface, the 670-km discontinuity, the core-mantle boundary, and the inner core boundary. These represent, on the same scale as the other kernels, the effect of a boundary deflection equal to 1% of the Earth's radius. The splitting functions are plotted in the same fashion as those in Figures 3–6. In this and in the following figures we display modes with similar differential kernels. The modes shown here show predominant sensitivity to v_P structure in the lower mantle and essentially vanishing sensitivity below the core-mantle boundary.

Fig 6.

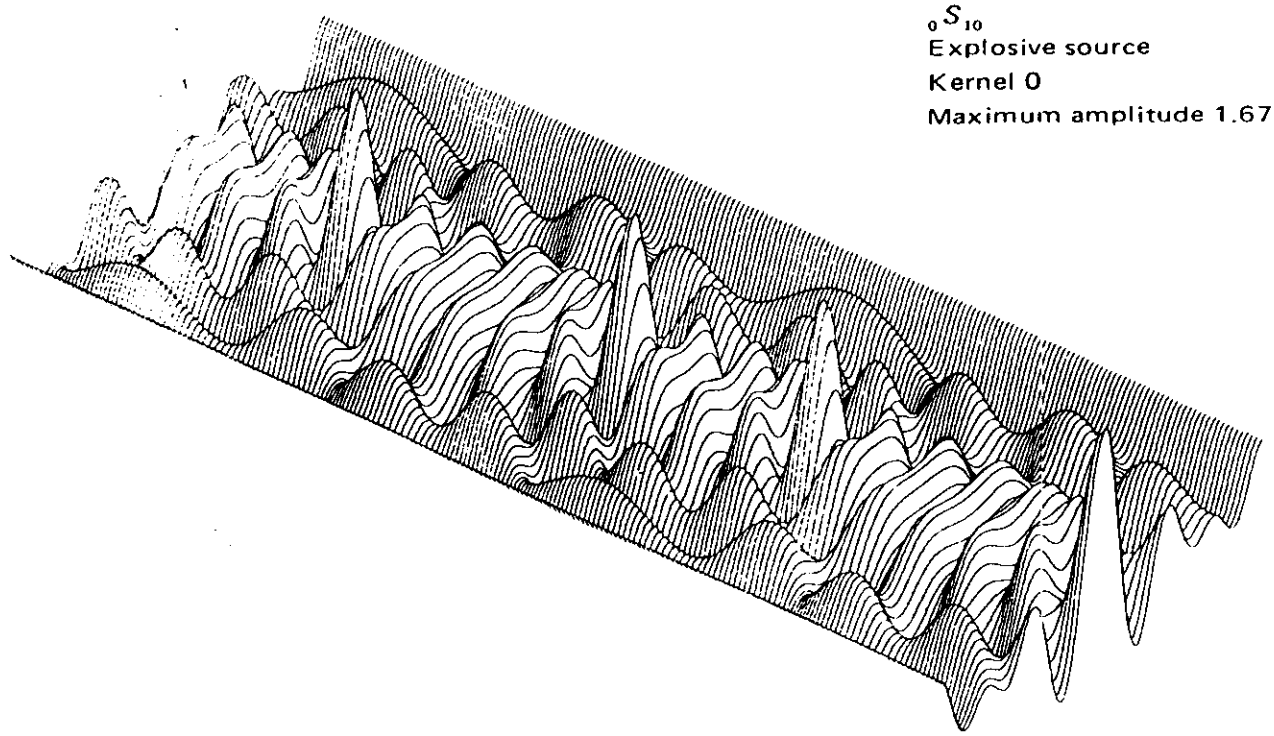
$_0S_{10}$
Explosive source
Kernel 0
Maximum amplitude 1.67

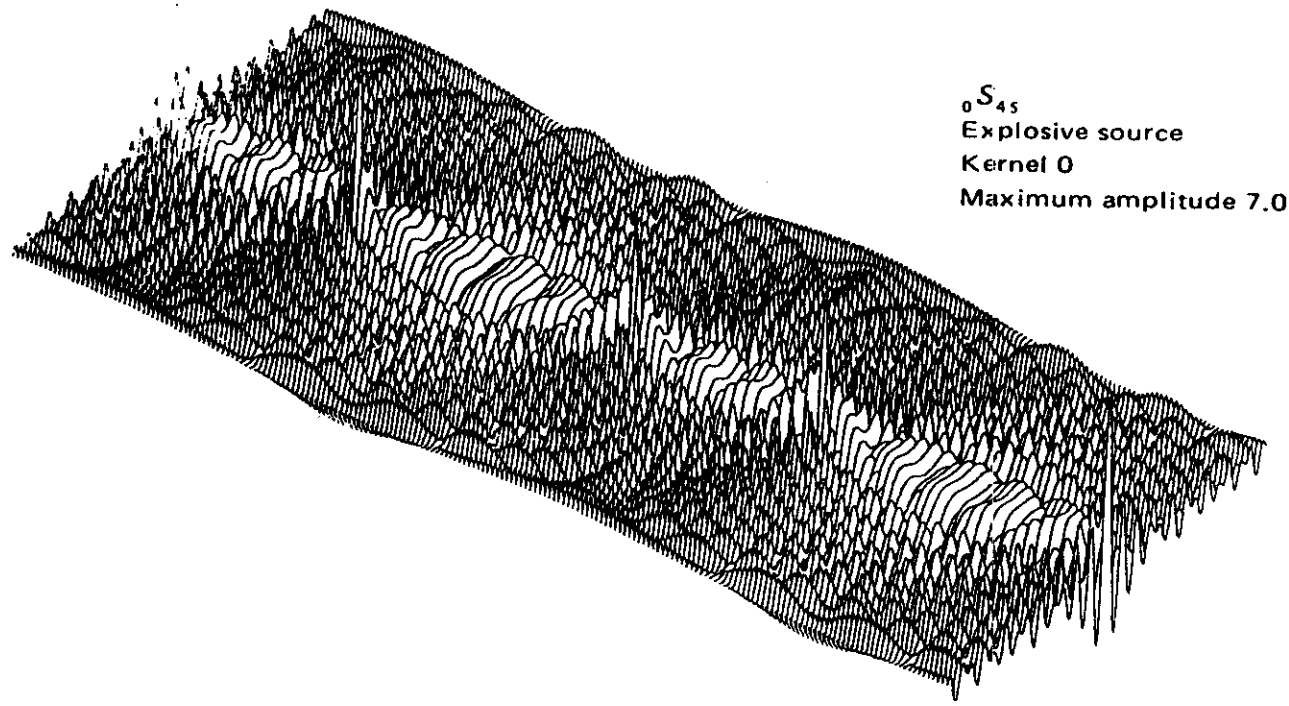
$_0S_{45}$
Explosive source
Kernel 0
Maximum amplitude 7.01

Fig 7.

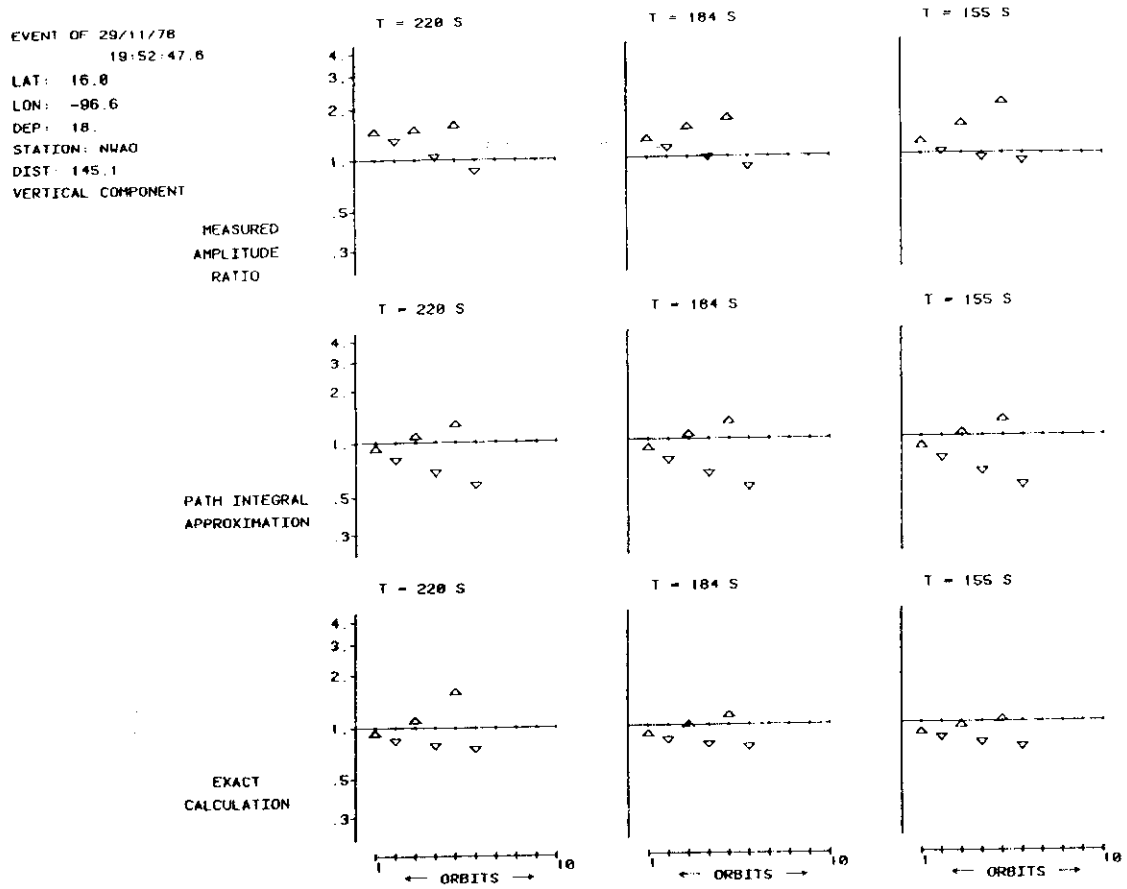

(a)

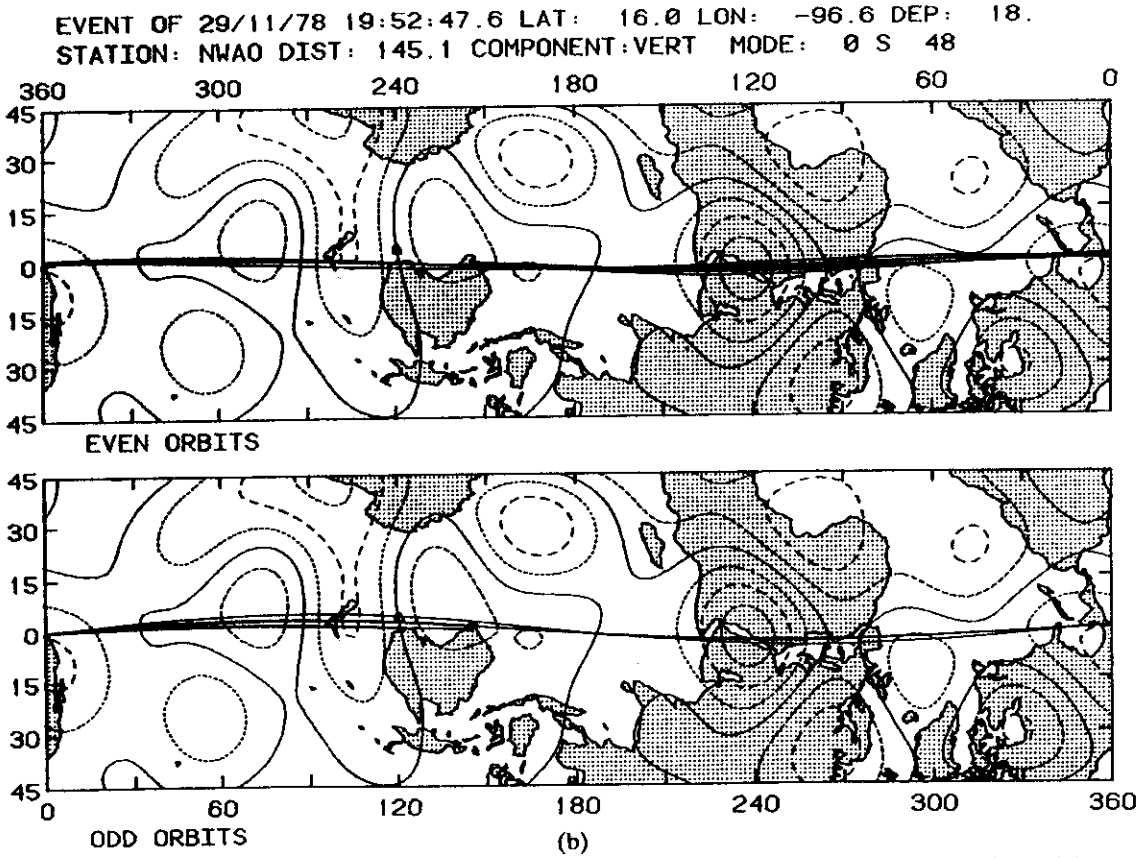

(b)

(a) Amplitude measurements (top row) as a function of orbit number, together with model calculations based upon the path integral approximation (middle row) and exact ray tracing (bottom row); the model calculations make use of the model M84C of Woodhouse & Dziewonski (1984). (b) The paths followed by the orbits of Fig. 3(a); all even orbits (top panel) and odd orbits (bottom panel) are superimposed.

Fig 8.

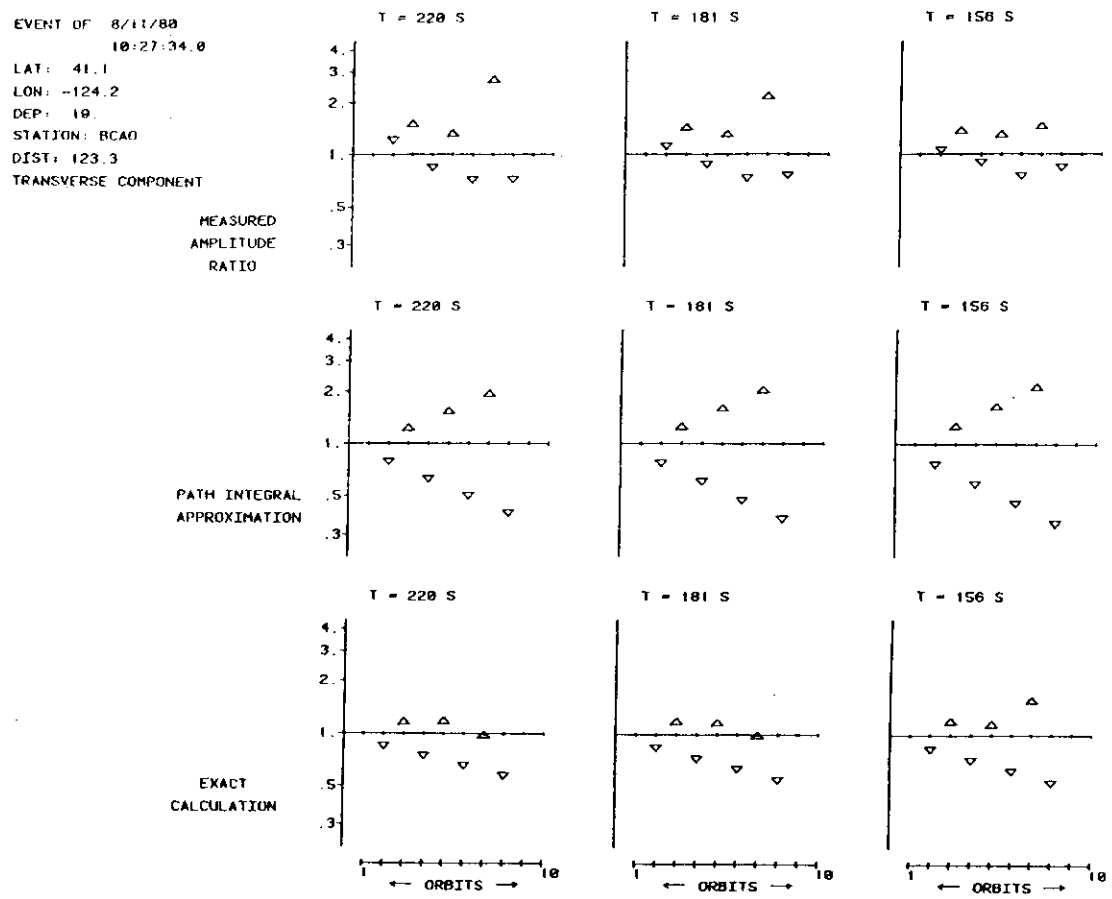

(a)

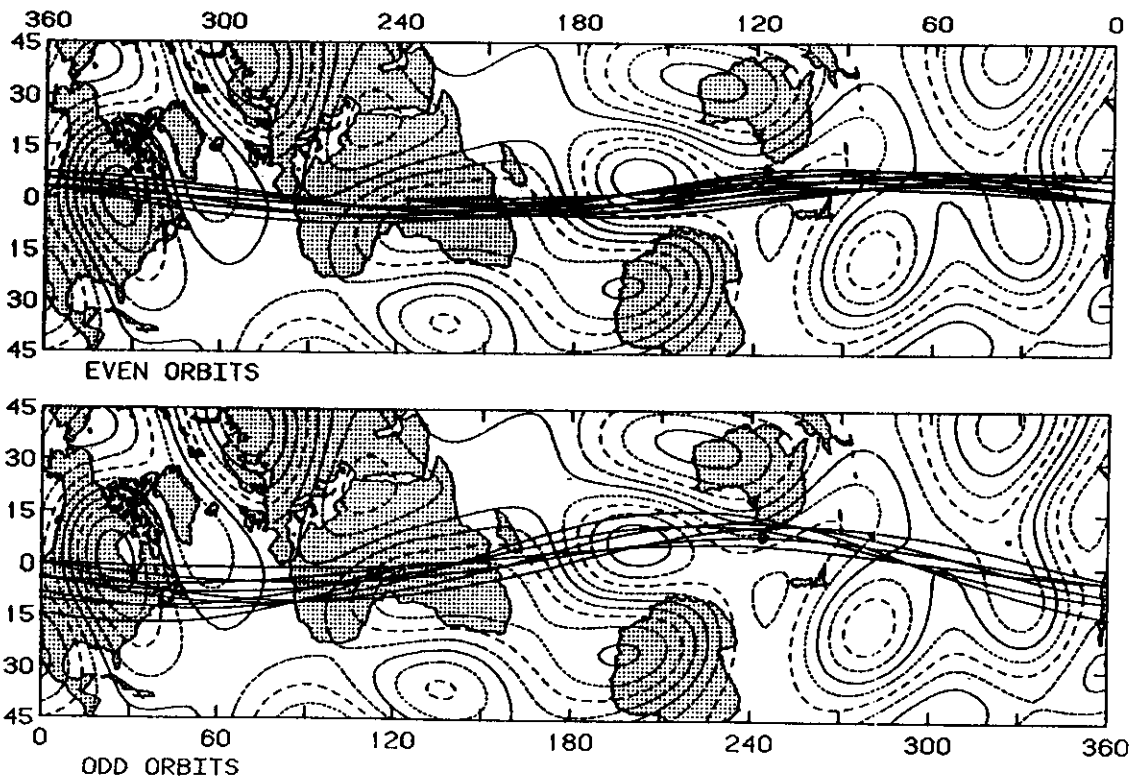

(b)

(a) Amplitude measurements and model calculations. See caption to Fig. 3(a). (b) The paths followed by the orbits of Fig. 4(a).

Fig 9.